Received: 16 April 2020 | Revised: 2 July 2020 | Accepted: 3 July 2020

DOI: 10.1111/bre.12492

ORIGINAL ARTICLE

Basin Research | IAS EAGE | WILEY

# The Svalbard Eocene-Oligocene (?) Central Basin succession: Sedimentation patterns and controls

**William Helland-Hansen**[1,2] | **Sten-Andreas Grundvåg**[3]

[1]Department of Earth Science, University of Bergen, Bergen, Norway

[2]UNIS, Longyearbyen, Norway

[3]Department of Geosciences, UiT - The Arctic University of Norway, Tromso, Norway

**Correspondence**
William Helland-Hansen, Department of Earth Science, University of Bergen, Bergen, Norway.
Email: william.helland-hansen@uib.no

**Funding information**
Research Council of Norway (support to Grundvåg/ARCEx; Research Centre for Arctic Petroleum Exploration), Grant/Award Number: 228107

**Abstract**

A synthesis has been undertaken based on regionally compiled data from the post early Eocene foreland basin succession of Svalbard. The aim has been to generate an updated depositional model and link this to controlling factors. The more than kilometer thick progradational succession includes the offshore shales of the Gilsonryggen Member of the Frysjaodden Formation, the shallow marine sandstones of the Battfjellet Formation and the predominantly heterolithic Aspelintoppen Formation, together recording the progressive eastwards infill of the foredeep flanking the West Spitsbergen fold-and-thrust belt. Here we present a summary of the paleo-environmental depositional systems across the basin, their facies and regional distribution and link these together in an updated depositional model. The basin-margin system prograded with an ascending shelf-edge trajectory in the order of 1°. The basin fill was bipartite, with offset stacked shelf and shelf-edge deltas, slope clinothems and basin floor fans in the western and deepest part and a simpler architecture of stacked shelf-deltas in the shallower eastern part. We suggest a foredeep setting governed by flexural loading, likely influenced by buckling, and potentially developing into a wedge top basin in the mature stage of basin filling. High-subsidence rates probably counteracted eustatic falls with the result that relative sea-level falls were uncommon. Distance to the source terrain was small and sedimentation rates was temporarily high. Time-equivalent deposits can be found outbound of Stappen High in the Vestbakken Volcanic Province and the Sørvestsnaget Basin 300 km further south on the Barents Shelf margin. We cannot see any direct evidence of coupling between these more southerly systems and the studied one; southerly diversion of the sediment-routing, if any, may have taken place beyond the limit of the preserved deposits.

**KEYWORDS**
Central Basin, Eocene, foreland basin, Paleogene, Spitsbergen, Svalbard

# 1 | INTRODUCTION

## 1.1 | Rationale and aims

The main sedimentary response to the Paleogene uplift of the West Spitsbergen Fold-and-Thrust Belt (WSFTB, Figure 1), the kilometer-scale thick progradational succession containing the Gilsonryggen Member of the Frysjaodden Formation (offshore), the Battfjellet Formation (shallow marine) and the Aspelintoppen Formation (continental) (Atkinson, 1963; Dallmann, 1999; Helland-Hansen, 1990; Kellogg, 1975; Major & Nagy, 1972; Nathorst, 1910; Steel, 1977; Steel, Dalland, Kalgraff, & Larsen, 1981; Steel et al., 1985) (Figures 2 and 3) has long been used as a scientific and educational laboratory. The extraordinary good exposures of both kilometer-scale as well as close-up facies-scale geometries excellently demonstrates aspects related to foreland basin sedimentation (Helland-Hansen, 1990), the spatial-temporal illustration of continental to submarine systems tracts (Johannessen & Steel, 2005), the coupling of seismic scale geometries to outcrops and

**Highlights**

- The studied succession accumulated in a foredeep zone of a foreland basin.
- The system drained from small catchments (500–1,000 km$^2$) with sediments accumulating close (<100 km) to the drainage divide.
- Progradation across the basin took place with an ascending shelf-edge trajectory.
- The succession is typified by a shingled architecture with limited lateral extent (3–6 km) of basinward-offset shallow marine lithosomes.
- Subsidence rates were high, probably preventing relative sea-level falls.

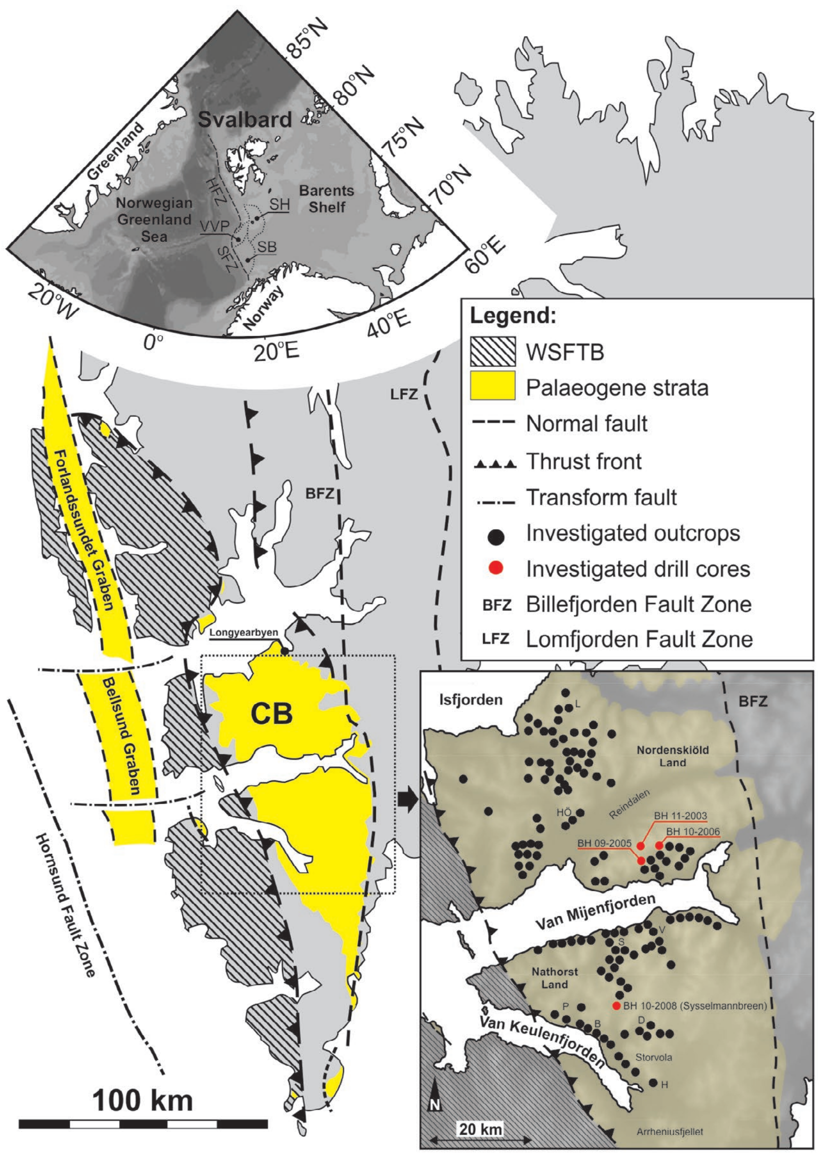


**FIGURE 1** Location of study area. Insert map shows location of logged sections that are compiled from our own data and publications, and MSc theses (for references, see paragraph "Data"). Geological map modified from Dallmann and Elvevold (2015) and Jochmann et al. (2019). HFZ: Hornsund Fault Zone; SFZ: Senja Fracture Zone; SB: Sørvestsnaget Basin; SH: Stappen High; VVP: Vestbakken Volcanic Province; WSFTB: West Spitsbergen Fold-and-thrust Belt; CB: Central Basin; L: Lars Hiertafjellet; S: Sven Nilssonfjellet; V. Vengefjellet; P: Pallfjellet; B: Brogniartfjella; D: Drevfjellet; H: Hyrnestabben

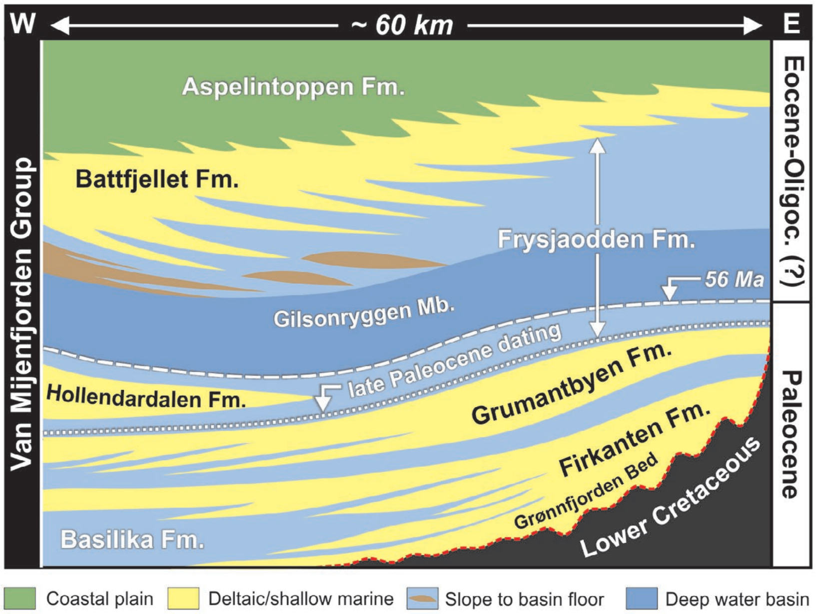


**FIGURE 2** Stratigraphy of the Central Basin Paleogene succession. Modified from Grundvåg, Johannessen, et al., 2014

subsurface (Helland-Hansen, Helle, & Sunde, 1994; Johannessen et al., 2011; Johansen, Granberg, Mellere, Arntsen, & Olsen, 2007), the process understanding of clinoform deposition and the link between coastal sedimentation and basin floor mass-gravity deposition (Deibert, Benda, Løseth, Schellpeper, & Steel, 2003; Steel & Olsen, 2002). More than 10 MSc theses and 30 publications have emanated from studies of this succession over the last 15 years and more than thousand students and numerous oil-company field excursions have visited the succession to gain knowledge about the abovementioned factors and relate them to subsurface systems.

Based on our own unpublished and published work and theses of MSc students we have supervised (see section *Data* below) and have given an updated and comprehensive overview of the paleogeographic and tectonostratigraphic development of the succession. Specifically, we will focus on development and distribution of the main depositional systems and how these are connected. We will discuss how the overall depositional trends together with information from new basin-scale maps (isopach, parasequence-number, paleocurrent-trend, clinoforms distribution, basin-floor fan distribution) relate to the overall basin filling and which controls were instrumental in determining the character of basin filling. Specifically, a comprehensive review of the basin type and extent, the basin forming processes, and the impact of subsidence, eustasy and sediment supply on the basin-fill history will be presented, adding to the more fragmented contributions on these aspects in the literature for this part of the Svalbard stratigraphy.

## 1.2 | Geological setting

The regressive megasequence of the combined Gilsonryggen Member, Battfjellet Formation and Aspelintoppen Formation (hereafter referred to as the GBA-unit) constitutes the upper part of the Paleogene Van Mijenfjorden Group in the Central Basin of Svalbard (Bruhn & Steel, 2003; Helland-Hansen, 1990; Steel et al., 1981, 1985) (Figures 2 and 3). The GBA-unit prograded from the West Spitsbergen Fold-and Thrust Belt (WSFTB) and eastwards into the flanking foreland basin from latest Paleocene and onwards and has a preserved thickness of more than 1,500 m (Helland-Hansen, 1990). The west to east transport direction is evidenced by paleocurrent data across the basin as well as the direction of sloping and thinning of clinothems in the western part of the basin (Helland-Hansen, 1990; Kellogg, 1975; Steel et al., 1981, 1985).

The formation of the Central Basin and WSFTB was a response to the development of a sheared margin along the western Barents Shelf as a result of the opening of the North-Atlantic in early Paleogene. The 750 km of dextral movement that was accommodated between the Eurasian and Greenland plates (Gaina, Gernigon, & Ball, 2009) gave a largely transtensive response at the southern part of the shear margin (the Senja Fracture Zone) (e.g. Faleide, Vågenes, & Gudlaugsson, 1993; Kristensen et al., 2018), whereas western Svalbard experienced 20–40 km of crustal shortening (Bergh, Braathen, & Andresen, 1997) as a result of transpression along the Hornsund Fault Zone (Figure 1).

The tectonic regime during the deposition of the oldest part of the Central Basin fill (Firkanten, Basilika and Grumantbyen formations, Figure 2) is debated, both strike-slip (Müller & Spielhagen, 1990), transtension (Dörr et al., 2019; Harland, Anderson, Manasrah, & Butterfield, 1997; Steel et al., 1981) and transpression (Bruhn & Steel, 2003; Jones et al., 2017) have been suggested. The westerly derived clastic wedge of the upper Paleocene Hollendardalen Formation below the GBA-unit indicates a drainage reversal relative to underlying

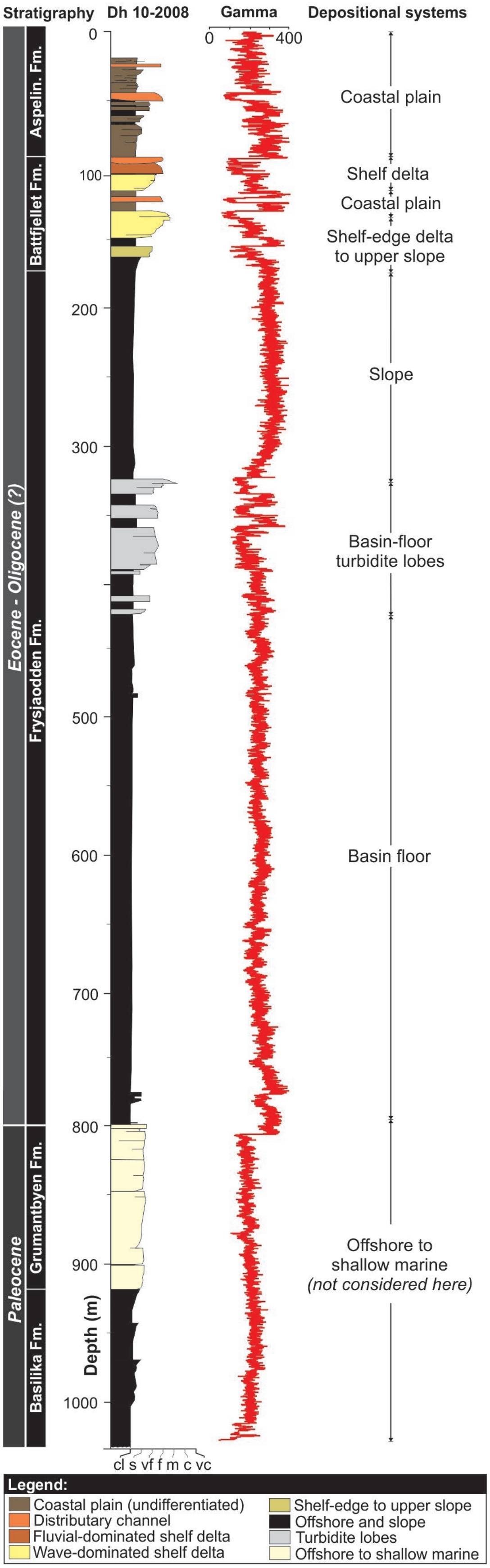


**FIGURE 3** The cored section of the Sysselmannbreen Well (cf. Figure 1 for location) showing lithology, gamma-ray and breakdown of depositional systems of the Frysjaodden, Battfjellet and Aspelintoppen Formations and their underlying Basilika and Grumantbyen formations. Modified from Grundvåg, Johannessen, et al., 2014

vclastic wedges and is assumed to be an early record of uplift in the west, whereas the GBA-unit itself represents the main sedimentary response (Helland-Hansen, 1990; Steel et al., 1981).

The syncline of the present Central Basin and its stratigraphic fill is the uplifted and eroded remnants of the final foredeep of the WSFTB (Dörr, Clift, Lisker, & Spiegel, 2013; Helland-Hansen, 1990) that existed prior to break-up and opening of the sea-way between Greenland and Norway commencing in the earliest Oligocene (Chron 13, Faleide et al., 1993; Lundin & Doré, 2002). Although debated, the poorly dated Forlandsundet Graben (Figure 1) northwest of the Central Basin is suggested by Kleinspehn and Teyssier (2016) to be a piggy-back basin within the WSFTB indicating progressive late Eocene–early Oligocene transition from oblique convergence to oblique divergence prior to the break-up. A similar development is inferred for the Bellsund Graben (Figure 1), which represent the southward extension of the Forlandsundet Graben (Blinova, Thorsen, Mjelde, & Faleide, 2009).

Time constraints on both structuring and accompanying foreland basin deposition are relatively limited. Only a few datings within the basin fill has been published; one gives a late Paleocene age based on dinoflagellate species within the lowermost part of the Frysjaodden Formation (below the Hollendardalen Formation, Figure 2) (cf. Manum & Throndsen, 1986, their Figure 6); another is dated to ca. 56 Ma at the level of the PETM (Paleocene-Eocene thermal maximum) close to the base of the GBA-unit using radiometric dating of bentonites in combination with astrochronology (Charles et al., 2011; Harding et al., 2011). Owing to the large thickness and the post late Paleocene age, most workers have assumed that the GBA-unit is dominantly of Eocene and possibly also of Oligocene age, however, this is not substantiated by biostratigaphic data. An early Eocene age has been suggested for the Aspelintoppen Formation based on comparison with other Arctic floras (Golovneva, 2010; Kvaček, 1994; Manum & Throndsen, 1986).

Tegner et al. (2011) and Piepjohn, von Gosen, and Tessensohn (2016) suggest that the WSFTB is equivalent to the Eurekan fold belts in North Greenland and Arctic Canada. Compression peaked at 47–49 Ma (mid Eocene) based on thermal resetting ages from Upper Cretaceous volcanic flows in North Greenland (Tegner et al., 2011). From

36 Ma and onwards the west Svalbard margin developed into a rifted margin (Eldholm, Sundvor, Myhre, & Faleide, 1984; Faleide et al., 1993) and was subject to rift shoulder uplift with continued erosion (Dimakis, Braathen, Faleide, Elverhøi, & Gudlaugsson, 1998; Dörr et al., 2013). In the late Neogene and Quaternary times, recurrent glaciations and erosion continued, with Svalbard currently being in the state of post-glacial isostatic uplift (e.g. Forman et al., 1995; Knies et al., 2009; Landvik et al., 1998).

Svalbard's paleolatitudal position was probably only a few degrees south of the present; Clifton (2012) suggests 75°N for the Central Basin during the deposition of the Aspelintoppen Formation. Temperatures were much warmer than today; Golovneva (2010) suggested a warm-temperate or moderately temperate climate with high precipitation rates in Svalbard in Paleogene times. Based on studies of plant material in the Aspelintoppen Formation, mean annual average temperatures were estimated to range from 9 to 17°C (Clifton, 2012; Golovneva, 2010; Uhl, Traiser, Griesser, & Denk, 2007).

Several studies have recorded outsized clasts, also within the Gilsonryggen Member in the lower part of the GBA-unit, which may indicate rafting by temporal sea ice (Dalland, 1977; Kellogg, 1975) or transport by driftwood (Birkenmajer & Narebski, 1963; Dalland, 1977). Rafting by sea ice is in accordance with some of the paleofloristic studies that also infer freezing temperatures during winter months (Golovneva, 2010; Uhl et al., 2007). Furthermore, the basin had low salinity because of large freshwater input from advancing deltas in a setting of high precipitation rates and elevated terrestrial runoff (Greenwood, Basinger, & Smith, 2010; Harding et al., 2011; Uhl et al., 2007). In summary, the climatic proxies together indicate a general temperate warm climate, possibly with strong seasonal or temporal variations.

### 1.2.1 | The basin fill

The preserved Central Basin foreland infill demonstrates a thinning of the marine part of the succession (the Hollendardalen Formation, the Gilsonryggen Member and the Battfjellet Formation) from the orogenic flank towards the basin, from more than 700 m in the west to 300 m in the eastern part (cf. Helland-Hansen, 1990). Present day erosion limits the thickness of this marine succession to be slightly above 700 m (Figure 4a) but it is reasonable to suggest that the succession had an initial thickness well above 800 m when extrapolating isopachs westwards into the deeply eroded areas (Figure 4b). The overlying continental strata (the Aspelintoppen Formation) define the present-day mountain tops in the basin area; hence its original thickness is unclear. The maximum preserved thickness is inferred to be more than 1,000 m on the south side of Van Mijenfjorden (Steel et el., 1981). According to recent vitrinite-reflectance-based overburden models by Marshall et al. (2015), the maximum depth of burial of coal in the Firkanten Formation in the Colesdalen area (central part of Nordenskiöld Land in the Central Basin) was in the order of 2.3 km. These data in combination with thickness maps by Bruhn and Steel (2003) for the Paleogene formation indicates, in the position of the maximum preserved thickness of the Aspelintoppen Formation on the south side of Van Mijenfjorden, about 500 m of removed overburden.

The upper part of the marine basin fill (the upper Gilsonryggen Member and the Battfjellet Formation) shows a distinct bi-partitioning into a western and eastern basin-segment with contrasting styles of basin fill (Helland-Hansen, 1990, 2010). Both sandstone clinothems 200–300 m high and basin-floor sandstones up to 60 m thick can clearly be seen along the mountainsides in the western part of the basin (Figure 5a). This is in contrast with the eastern part of the basin where no such features can be seen.

The sandstones of the Battfjellet and Aspelintoppen formations are generally poorly sorted lithic greywackes with a large fraction of rock fragments and organic matter (Helland-Hansen, 2010; Mansurbeg et al., 2012; Nysæther, 1966; Schlegel et al., 2013). The sand grain-size is typically not coarser than medium with very fine-grained sands constituting the volumetrically most important sand-fraction caliber (cf. Grundvåg, Helland-Hansen, Johannessen, Olsen, & Stene, 2014; Grundvåg, Johannessen, Helland-Hansen, & Plink-Björklund, 2014; Helland-Hansen, 2010). Occasionally, thin conglomeratic horizons may be present at the base of fluvial channels (Naurstad, 2014); however, this sediment caliber is negligible in volume relative to the finer grain sizes. Another characteristic feature of the succession is pervasive soft sediment deformation mostly due to vertical foundering (load structures), particularly in the lower to middle part of the Battfjellet Formation but also in the partly interfingering and overlying Aspelintoppen Formation (Grundvåg, Helland-Hansen, et al., 2014; Helland-Hansen, 2010; Naurstad, 2014; Steel et al., 1981).

## 1.3 | Data

Based on field data, our published literature and theses of MSc students we have supervised, thicknesses, paleocurrent data and facies-breakdown have been compiled from logged profiles (c.f. Helland-Hansen, 1985, 1990, 2010; Grundvåg, Johannessen, et al., 2014, Grundvåg, Helland-Hansen, et al., 2014, and MSc dissertations by Olsen, 2008; Stene, 2008; Gjelberg, 2010; Skarpeid, 2010; Osen, 2012; Naurstad, 2014; Jørgensen, 2015; Kongsgården, 2016; Broze, 2017; Skjærpe, 2017; Aamelfot, 2019). Figure 1

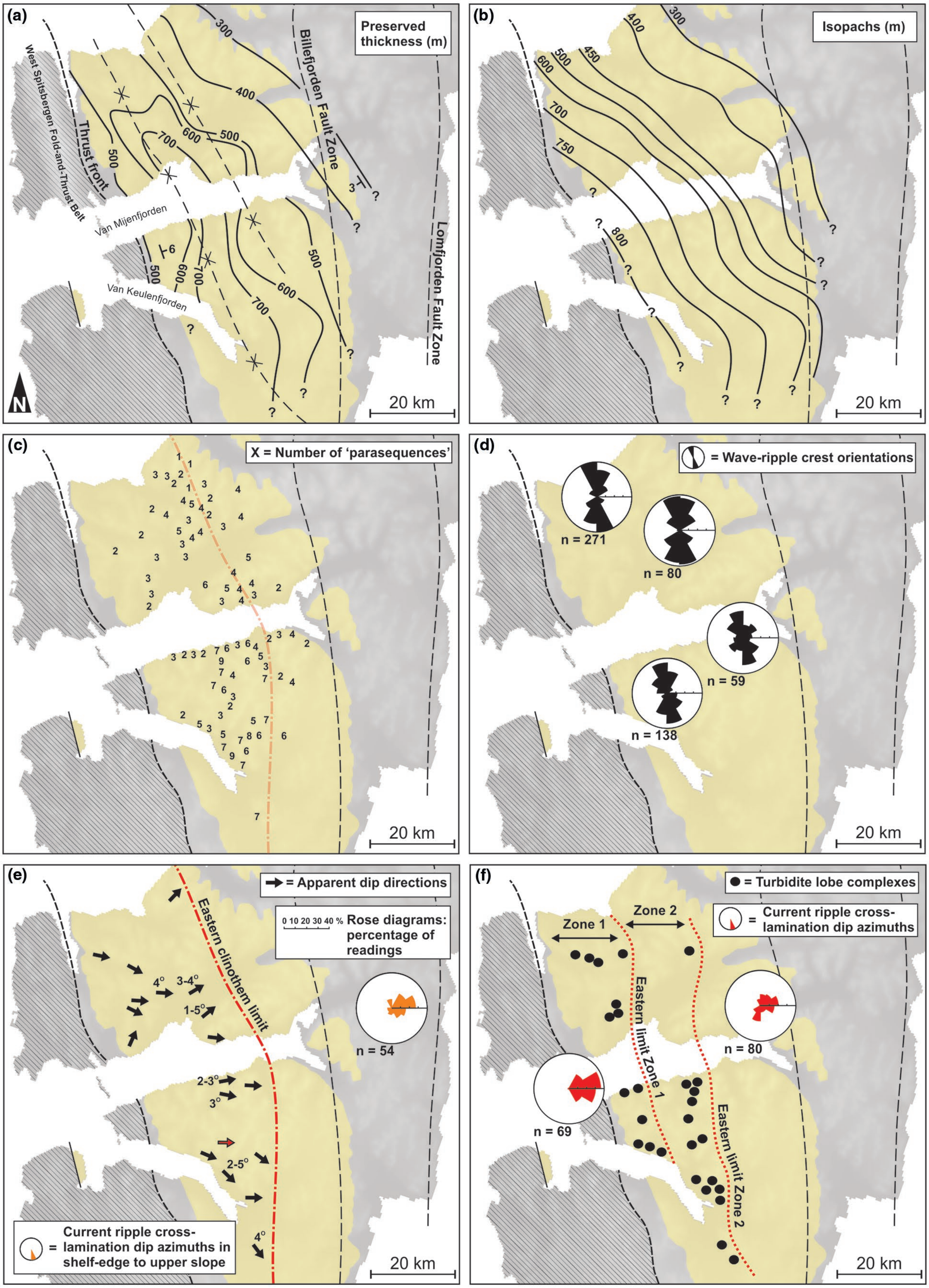
(a)
Preserved thickness (m)
West Spitsbergen Fold-and-Thrust Belt
Thrust front
Billefjorden Fault Zone
Lomfjorden Fault Zone
Van Mijenfjorden
Van Keulenfjorden
300
400
500
600
700
N
20 km
(b)
Isopachs (m)
300
400
450
500
600
700
750
800
20 km
(c)
X = Number of 'parasequences'
20 km
(d)
= Wave-ripple crest orientations
n = 271
n = 80
n = 59
n = 138
20 km
(e)
= Apparent dip directions
0 10 20 30 40 % Rose diagrams: percentage of readings
Eastern clinothem limit
4°
3-4°
1-5°
2-3°
3°
2-5°
n = 54
= Current ripple cross-lamination dip azimuths in shelf-edge to upper slope
20 km
(f)
= Turbidite lobe complexes
= Current ripple cross-lamination dip azimuths
Zone 1
Zone 2
Eastern limit Zone 1
Eastern limit Zone 2
n = 80
n = 69
20 km

**FIGURE 4** (cf. Figure 1 for map outline, data in maps A-F compiled from MSc theses and our own data and publications, for references, see paragraph "Data"). (a) Preserved thickness of the of the combined Hollendardalen Formation, Gilsonryggen Member and Battfjellet Formation; (b) Composite isopach thickness of the combined Hollendardalen Formation, Gilsonryggen Member and Battfjellet Formation (inferred thicknesses in areas where present day erosion extends into the Battfjellet and underlying formations); (c) Number of parasequences (>5 m) in the Battfjellet Formation at logged localities; (d) Wave-ripple crest orientations compiled from logged sections and summarized for four sub-areas; (e) Dip azimuths of current-ripple cross-lamination at shelf-edge to upper slope positions (rose diagram) and apparent clinoform dip directions/slope angles. Note that clinoforms are concentrated in the western part of the study area; (f) Location of logged sections with turbidite lobe complexes (note that these are concentrated in two zones) and dip azimuths of current-ripple cross-lamination (for Zone 1 (left) and Zone 2 (right), respectively). Yellow colour in maps (a)–(f) denotes outline of Central Basin

shows position of the vertical profiles and Figure 4 shows compiled thicknesses and paleocurrent data. For examples of sedimentary logs we refer to Figures 3 and 6. For a regional overview of study areas and logs compiled from the different sources, see Figure S1. The general facies succession, as well as the detailed depositional architecture of some clinothems is thoroughly documented in previous papers (e.g. Grundvåg, Helland-Hansen, et al., 2014; Grundvåg, Johannessen, et al., 2014; Helland-Hansen, 1992; Helland-Hansen, 2010; Johannessen & Steel, 2005; Mellere, Breda, & Steel, 2003; Petter & Steel, 2006; Steel, 1977; Uroza & Steel, 2008) and will not be reiterated here. In the following we will go through individual basin-scale depositional systems moving from continental to offshore and basinal areas, briefly describe their facies development and summarize their spatial distribution as basis for a new regional synthesis of the basin fill history and its controls.

## 2 | DEPOSITIONAL SYSTEMS

### 2.1 | Coastal plain

Coastal plain sediments (the Aspelintoppen Formation, Clifton, 2012; Naurstad, 2014; Steel et al., 1981) locally interfinger with and cap the underlying shelf-delta sediments (below) and extend all the way to mountain tops (Figure 5a). Depending of the position within the Central Basin and the height of the mountains, the thickness of the Aspelintoppen Formation is highly variable, but as noted above, it may be as much as 1,000 m in the central part of the basin (Steel et al., 1981).

Inter-channel floodplain deposits are dominating (Figures 6a and 7a,b), but ribbon-shaped channel sandstone bodies which are a few to maximum 15 m thick with limited lateral extent (tens to a few hundred meters) are variably present (Figures 6a and 7c) (Naurstad, 2014). These are typically single and multiple stacked with erosive, locally conglomeratic bases or scours (with frequent mud-clasts and wood fragments) and crude fining upwards and display pervasive soft sedimentary deformation. The channels are interpreted as relatively short-lived low-sinuosity channels (Figure 8) (Grundvåg, Helland-Hansen, et al., 2014; Naurstad, 2014).

Inter-channel floodplain deposits (Figures 6a and 7a,b) are dominated by sheet-formed units 0.5–5 m thick. These typically consist of heterolithic deposits grading upwards into very fine to fine-grained sandstones in coarsening- and thickening-upwards units, sometimes interrupted by crude fining-upwards channelized elements 1–3 m thick in medium to very fine-grained sandstones (Figure 7c). The coarsening- and thickening upwards motifs are interpreted in terms of levee and crevasse splay progradation; the fining-upward motifs as crevasse channels (Naurstad, 2014). In addition, 1–5 m thick units of finely laminated mudstones with abundant leaf fragments, siltstones and very fine-grained sandstones as well as thin coal layers (Figure 7a) represent a more quiescent overbank floodplain environment. For detailed facies-breakdown we refer to Grundvåg, Helland-Hansen, et al. (2014) and Naurstad (2014).

According to data from Brogniartfjella in Van Keulenfjorden (cf. Figure 1) the facies pattern of the coastal plain depositional system show remarkably minor gross environmental variations upwards in the succession apart from a relatively limited zone (max. 10 m) in the basal part that shows clear brackish influence from the constituent trace fossil assemblages (Naurstad, 2014); the remaining upper part being devoid of tidal or brackish water influence. Clifton (2012), in a dissertation about the Eocene flora of Svalbard, studied the same succession at Brogniartfjella and could not find evidence of tidal influence. Grundvåg, Helland-Hansen, et al., 2014 recognize facies deposited in brackish-water environments, but identifies no clear tidal signatures in the coastal plain succession in the 50 m cored lower part of the Aspelintoppen Formation in the nearby Sysselmannbreen well (cf. Figure 1). The only exception is bi-directional cross-strata occurring in the up-dip part of some of the shelf-delta parasequences (below) that interfinger with or are encapsulated within the coastal plain facies. These observations are in contrast with previous publications from the same area that have inferred strong tidal influence at multiple levels of the coastal plain system (apparently confined to incised valleys; e.g. Plink-Björklund, 2005), also at the higher stratigraphic levels of the Aspelintoppen Formation.

The system as a whole is suggested to be the result of high subsidence in combination with high sedimentation rates promoting vertical aggradation and frequent channel-avulsion

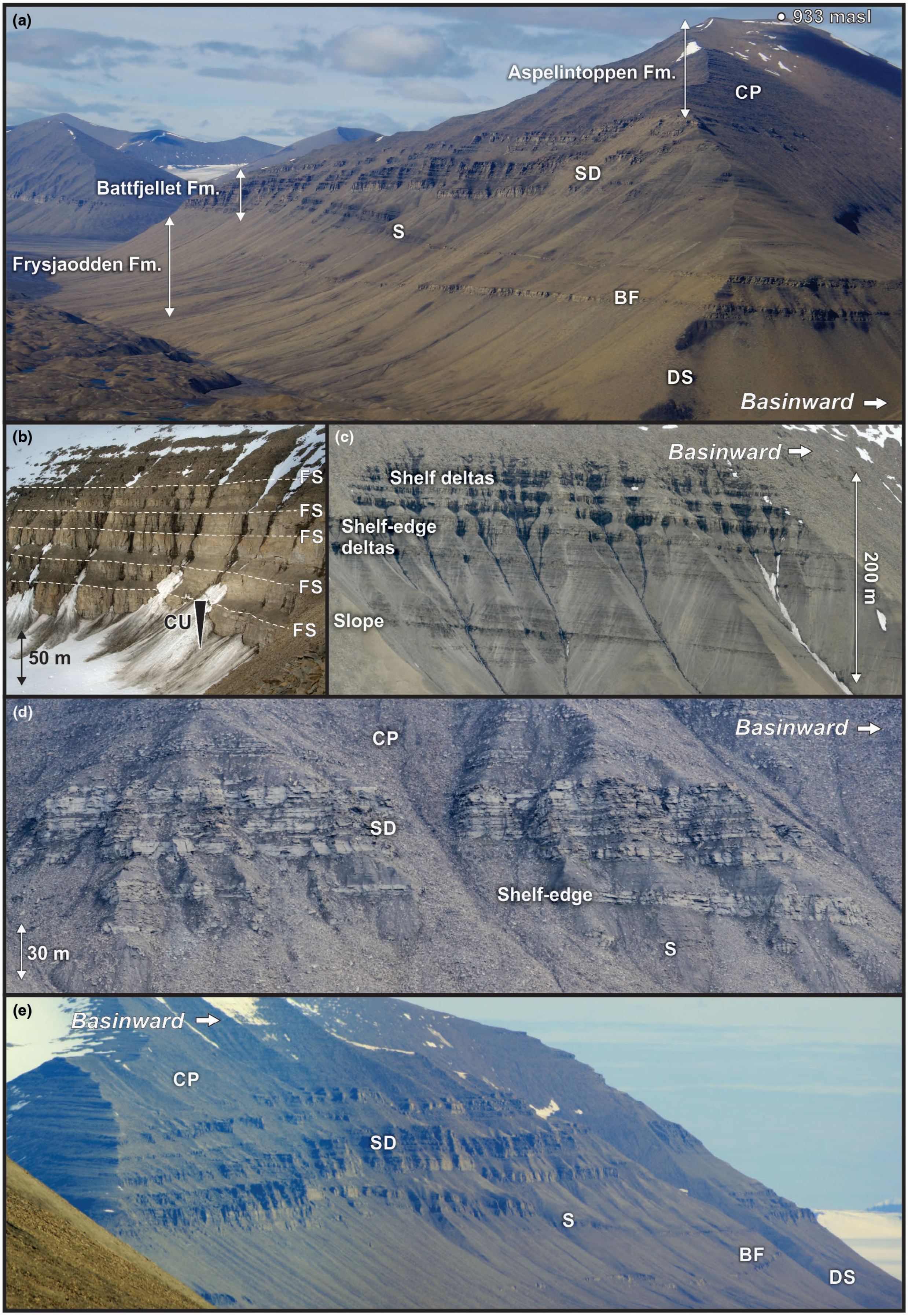

(a)
933 masl
Aspelintoppen Fm.
CP
Battfjellet Fm.
SD
S
Frysjaodden Fm.
BF
DS
Basinward
(b)
FS
FS
FS
FS
CU
FS
50 m
(c)
Basinward
Shelf deltas
Shelf-edge deltas
200 m
Slope
(d)
CP
Basinward
SD
Shelf-edge
30 m
S
(e)
Basinward
CP
SD
S
BF
DS

**FIGURE 5** Overview photos of depositional systems within the GBA-unit: (a) The mountain Storvola in Van Keulenfjorden viewed towards northwest showing coastal plain (CP), shelf-delta (SD), slope (S), basin floor (BF) and deepwater shale (DS) depositional systems (width of mountain about 6km); (b) stacked coarsening-upwards (CU) shelf-delta parasequences with intervening flooding surfaces (FS, stipled lines) at Drevfjellet; (c) transition from slope to shelf-edge deltas and shelf-deltas at the south side of Sven Nilssonfjellet; (d) superimposed slope, shelf-edge delta, shelf-delta and coastal plain sediments at Brogniartfjella, Van Keulenfjorden. Note sloping shelf-edge delta wedge; (e) Storvola in Van Keulenfjorden viewed towards southeast showing coastal plain (CP), shelf-delta (SD), slope (S), basin floor (BF) and deepwater shale (DS) depositional systems. For location of photos see Figure 1

(Naurstad, 2014). The interpreted avulsive nature of the fluvial system is verified and distinctly reflected in the downstream and time-equivalent shelf deltaic deposits in the Battfjellet Formation (see shelf-delta, below).

#### 2.1.1 | Regional distribution of coastal plain depositional system

The regional distribution and thickness of the coastal plain depositional system is primarily a function of the present-day relief of the landscape and the position within the broad syncline of the Central Basin. The thickest preserved successions are present in the axial parts of the Central Basin (Steel et al., 1981) with thinning and eventually absence towards the flanks of the trough. Specifically, the thinning or absence of the Aspelintoppen Formation only reflects modern day erosion; no primary thinning, pinchout or erosion of the formation has been recorded, apart from smaller scale variations caused by intrinsic sedimentological processes (e.g. localized channel erosion).

### 2.2 | Shelf-delta

Shelf-deltas are typically expressed as a single or repeated shallowing upwards "parasequences" (sensu Van Wagoner, Mitchum, Campion, & Rahmanian, 1990) grading from mudstones, siltstones and very fine grained sandstones in heterolithic packages up to very fine, fine or medium-grained sandstones (Figures 5b–d, 6b and 7d) (Grundvåg, Helland-Hansen, et al., 2014; Helland-Hansen, 2010). Individual units often terminate upwards without reaching coastal plain lithosomes, however, exceptions to this occur and the uppermost parasequence will always transition into coastal plain lithosomes indicating the change from the marine Battfjellet Formation to the continental Aspelintoppen Formation. The common upwards termination of parasequences in the marine lithosome is an expression of short progradation distance relative to the wedge-out distance of each parasequence beyond the most basinward shoreline position (Helland-Hansen, 2010). Thickness of individual parasequences ranges from 10,201,330 m; where multiple units are stacked, they are separated by marine flooding surfaces (sensu Van Wagoner et al., 1990; Figure 5b). The parasequences possess sedimentary structures pointing to tempestite deposition in the lower offshore-transition part of the succession (hummocky-cross-stratification and ball-and-pillow structures) and deposition indicating more continuous wave and shallow-marine current action, locally with tidal influence, in the overlying shoreface to foreshore part of the succession (Figure 7d–f). The latter part is expressed by alternating sets of wave-ripple lamination and plane-parallel lamination passing upwards into low-angle-, through- and planar-cross stratification (Figure 6b; Gjelberg, 2010; Helland-Hansen, 2010). Wave-ripple crests have a broadly N-S orientation across the entire basin (Figure 4d). Occasionally units show tidal influence in the uppermost part (co-sets of bipolar cross-stratification; Figure 6c) or are cut by distributary fluvial systems (upper part of lower parasequence shown in Figure 6b). Detailed facies break-down is given in Helland-Hansen, 2010, and Grundvåg, Helland-Hansen, et al., 2014.

#### 2.2.1 | Regional distribution of shelf-delta depositional system

The shelf-delta parasequences are widely distributed across the entire study area. They are conspicuous as the stratigraphically youngest main cliff-forming landscape element in Svalbard, and they constitute volumetrically the most important sand-sink in the basin. At outcrop scale they typically have a horizontal-tabular expression (Figure 5b–d); a result of sand distribution being conditioned by the vertical energy-zonation in the water-column as opposed to the clinothems of the slope segment that is the result of gravity emplacement *along* dipping bedding planes (below) (Helland-Hansen, 2010). Their progradational distance is typically in the range of 3–6 km and they probably extend less than 20km along depositional strike (Grundvåg, Helland-Hansen, et al., 2014). The number of stacked parasequences is highly variable, also over short (kilometer) distances (Figure 4c), but they seem to be more abundant in the western part of the basin where subsidence rates have been higher and vertical stacking are more pronounced. The highly variable number of stacked units points to elongated deltaic lobes that switched laterally as the deltas prograded into and filled the basin. This, in combination with strong evidence of wave reworking suggested by the sedimentary structures, made Helland-Hansen (2010)

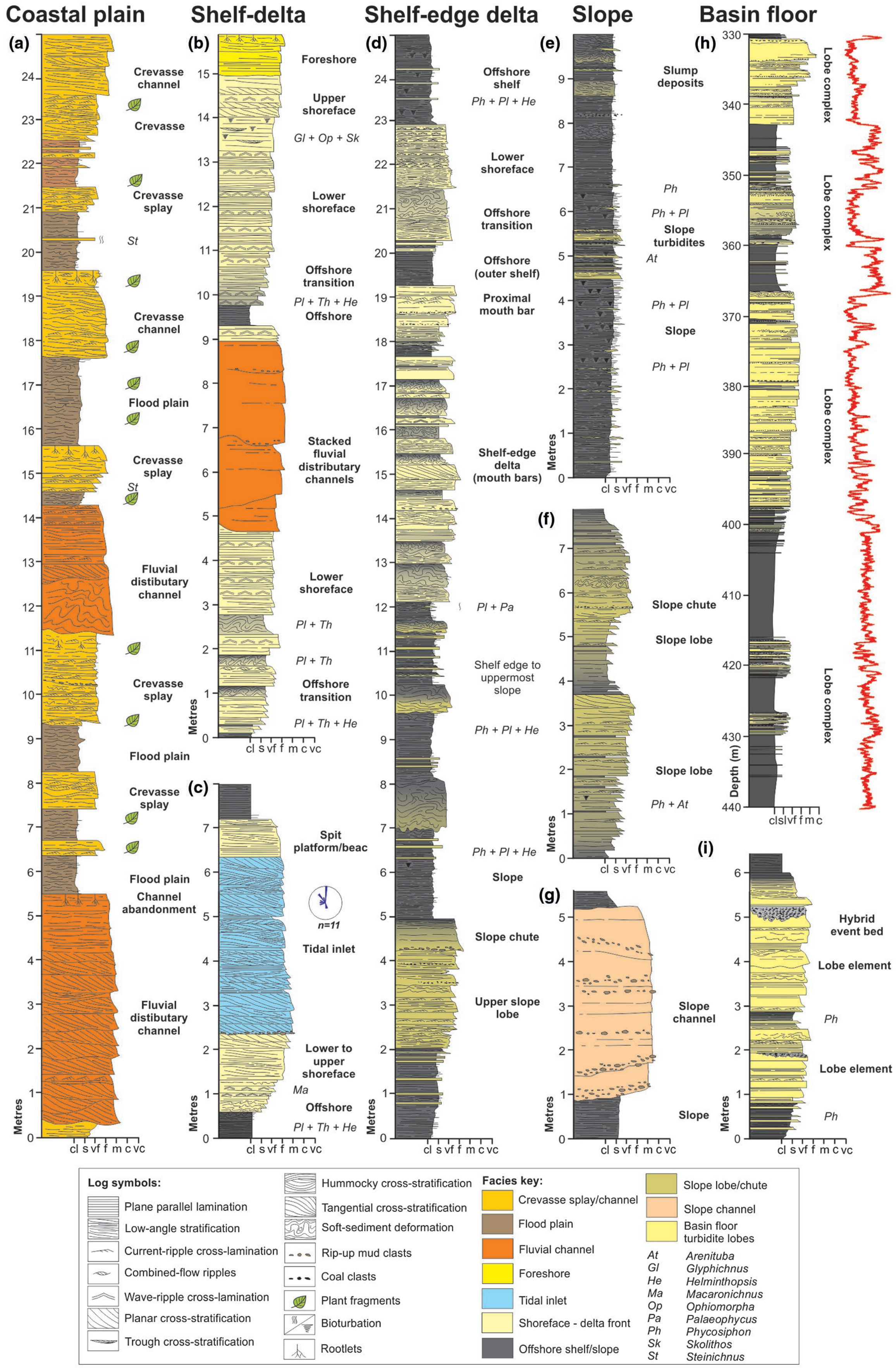
Coastal plain
Shelf-delta
Shelf-edge delta
Slope
Basin floor
(a)
Crevasse channel
Crevasse
Crevasse splay
St
Crevasse channel
Flood plain
Crevasse splay
St
Fluvial distibutary channel
Crevasse splay
Flood plain
Crevasse splay
Flood plain
Channel abandonment
Fluvial distibutary channel
(b)
Foreshore
Upper shoreface
Gl + Op + Sk
Lower shoreface
Offshore transition
Pl + Th + He
Offshore
Stacked fluvial distributary channels
Lower shoreface
Pl + Th
Pl + Th
Offshore transition
Pl + Th + He
(c)
Spit platform/beac
n=11
Tidal inlet
Lower to upper shoreface
Ma
Offshore
Pl + Th + He
(d)
Offshore shelf
Ph + Pl + He
Lower shoreface
Offshore transition
Offshore (outer shelf)
Proximal mouth bar
Shelf-edge delta (mouth bars)
Pl + Pa
Shelf edge to uppermost slope
Ph + Pl + He
Ph + Pl + He
Slope
Slope chute
Upper slope lobe
(e)
Slump deposits
Ph
Ph + Pl
Slope turbidites
At
Ph + Pl
Slope
Ph + Pl
(f)
Slope chute
Slope lobe
Slope lobe
Ph + At
(g)
Slope channel
Slope
(h)
Lobe complex
Lobe complex
Lobe complex
Lobe complex
Depth (m)
(i)
Hybrid event bed
Lobe element
Ph
Lobe element
Ph
Metres
cl s vf f m c vc
Log symbols:
Plane parallel lamination
Low-angle stratification
Current-ripple cross-lamination
Combined-flow ripples
Wave-ripple cross-lamination
Planar cross-stratification
Trough cross-stratification
Hummocky cross-stratification
Tangential cross-stratification
Soft-sediment deformation
Rip-up mud clasts
Coal clasts
Plant fragments
Bioturbation
Rootlets
Facies key:
Crevasse splay/channel
Flood plain
Fluvial channel
Foreshore
Tidal inlet
Shoreface - delta front
Offshore shelf/slope
Slope lobe/chute
Slope channel
Basin floor turbidite lobes
At Arenituba
Gl Glyphichnus
He Helminthopsis
Ma Macaronichnus
Op Ophiomorpha
Pa Palaeophycus
Ph Phycosiphon
Sk Skolithos
St Steinichnus

**FIGURE 6** Logs through the different depositional systems in the GBA-unit showing grain-sizes, sedimentary structures, trace fossils and environmental interpretations (locations of logs (see Figure 1): (a) Vengefjellet, (b) south side of Sven Nilssonfjellet, (c) western part of Brogniartfjella; (d) western Sven Nilssonfjellet, (e) Pallfjellet, (f) western Sven Nilssonfjellet, (g) Sysselmannbreen well, (h) Sysselmannbreen well and (i) Hyrnestabben)

propose a fluvio-wave interaction type of delta (Figure 8a,b). The parasequences may (Figure 5a,d,e) or may not extend laterally into shelf-edge and slope depositional systems, depending on their shelf-transit distance and position in basin; specifically it is only in the western basin-segment parasequences may link up with slope and turbidite lobe deposits together constituting large-scale (up to 350 m high) clinothems (cf. Figure 9) (Helland-Hansen, 2010).

## 2.3 | Shelf-edge delta and upper slope

Stratigraphically, this depositional system is positioned down-dip and seaward of shelf delta depositional system (above) and up-dip and landward of the slope depositional system (below). The shelf-edge delta and upper slope depositional system together form up to 5 km long and up to 80 m thick basinward thinning sandstone-dominated wedges or clinothems (see also Helland-Hansen, 1992; Steel et al., 2000; Plink-Bjorklund, Mellere, & Steel, 2001; Mellere, Plink-Bjorklund, & Steel, 2002; Steel & Olsen, 2002; Johannessen & Steel, 2005; Plink-Björklund & Steel, 2005; Pontén & Plink-Björklund, 2009) (Figures 5a,d,e and 6d).

Internally, the depositional system is characterized by 2–18 m thick coarsening- and thickening-upward successions of alternating thin-bedded mudstones, siltstones and very fine-grained sandstones forming heterolithic sheet-formed units in the lower part passing laterally upward into sharp-based, amalgamated, medium- to thick-bedded, fine- to coarse-grained sandstones (Figure 6d,g; Mellere et al., 2002; Plink-Björklund & Steel, 2005; Petter & Steel, 2006). In the lower part of the coarsening-upward units, plane-parallel lamination and current-ripple cross-lamination is common (including climbing sets); locally with abundant soft-sediment deformation (Figure 7g). Individual beds in the upper part are commonly wedge shaped, normally to non-graded, plane-parallel to low-angle laminated, or locally planar cross-stratified, in places forming sigmoidal bars (sensu Mutti, Davoli, Tinterri, & Zavala, 1996) 1–2.5 m thick (Grundvåg, Helland-Hansen, et al., 2014). Amalgamated sandstone units, 0.5–3 m thick, incises the sigmoidal bars in places. For detailed facies-breakdown, see Plink-Bjorklund et al. (2001) and Mellere et al. (2002).

Based on its stratigraphic position, the coarsening- and thickening-upward stacking pattern and the internal facies architecture dominated by traction and current-generated structures, this depositional system is interpreted as fluvial-dominated mouth bars deposited at the shelf-edge and upper slope (Figure 8). Thus, the heterolithic lower segment is interpreted as distal delta front deposits locally extending onto the slope, whereas the more amalgamated upper segment containing sigmoidal bars are interpreted as flood-dominated proximal delta front and mouth bar deposits (Grundvåg, Helland-Hansen, et al., 2014; Mellere et al., 2002).

## 2.4 | Slope

This depositional system contains both mudstone dominated slope deposits and sandstone dominated slope lobe deposits (distal part of clinothems) (Grundvåg, Johannessen, et al., 2014) and occur downdip and below shelf-edge delta and upper slope depositional system (above) and updip and above the flat lying turbidite lobe depositional system (below) (Figure 5a,c,e).

The slope deposits occur at a 100–150 m thick interval and comprises mainly laminated, soft-sediment deformed and structureless mudstone to siltstone with subordinate thin-bedded very fine-grained sandstones (Figure 6e). The sandstone beds are sharp based, normally graded, locally inclined and occasionally contains plane-parallel lamination and current-ripple cross-lamination. Based on its mudstone-dominated character, its stratigraphic position above basin-floor deposits, and by the high frequency of gravity-driven soft-sediment deformed beds (i.e. slumped beds), this facies association is interpreted to represent deposition on a relatively steep slope (Grundvåg, Johannessen, et al., 2014).

The sandy slope lobe deposits consist of thin- to thick-bedded siltstones and very fine- to fine-grained sandstones that alternates with thin intervals of mudstones, together forming heterolithic, sandstone-dominated, sheet-like bed-sets 2–4 m thick (Figures 6f and 7h). Individual sandstone beds are tabular and normally graded, locally exhibiting plane parallel lamination and current ripple cross-lamination. The sheet-like units stack vertically into basinward-thinning wedges up to c. 20 m thick and 1–3 km long, constituting clinothems which dip basinward with gradients of 2–5° (Figures 4e and 5a,e; Johannessen & Steel, 2005; Mellere et al., 2002; Petter & Steel, 2006). Internally, these wedges are coarsening- and thickening-upward or fining- and thinning-upward (Figure 6f). Up-dip toward the shelf-edge, the wedges show a landward increase in both sandstone content and bed-set amalgamation as they pass into the shelf edge and upper slope depositional system (Mellere et al., 2002). The frequency

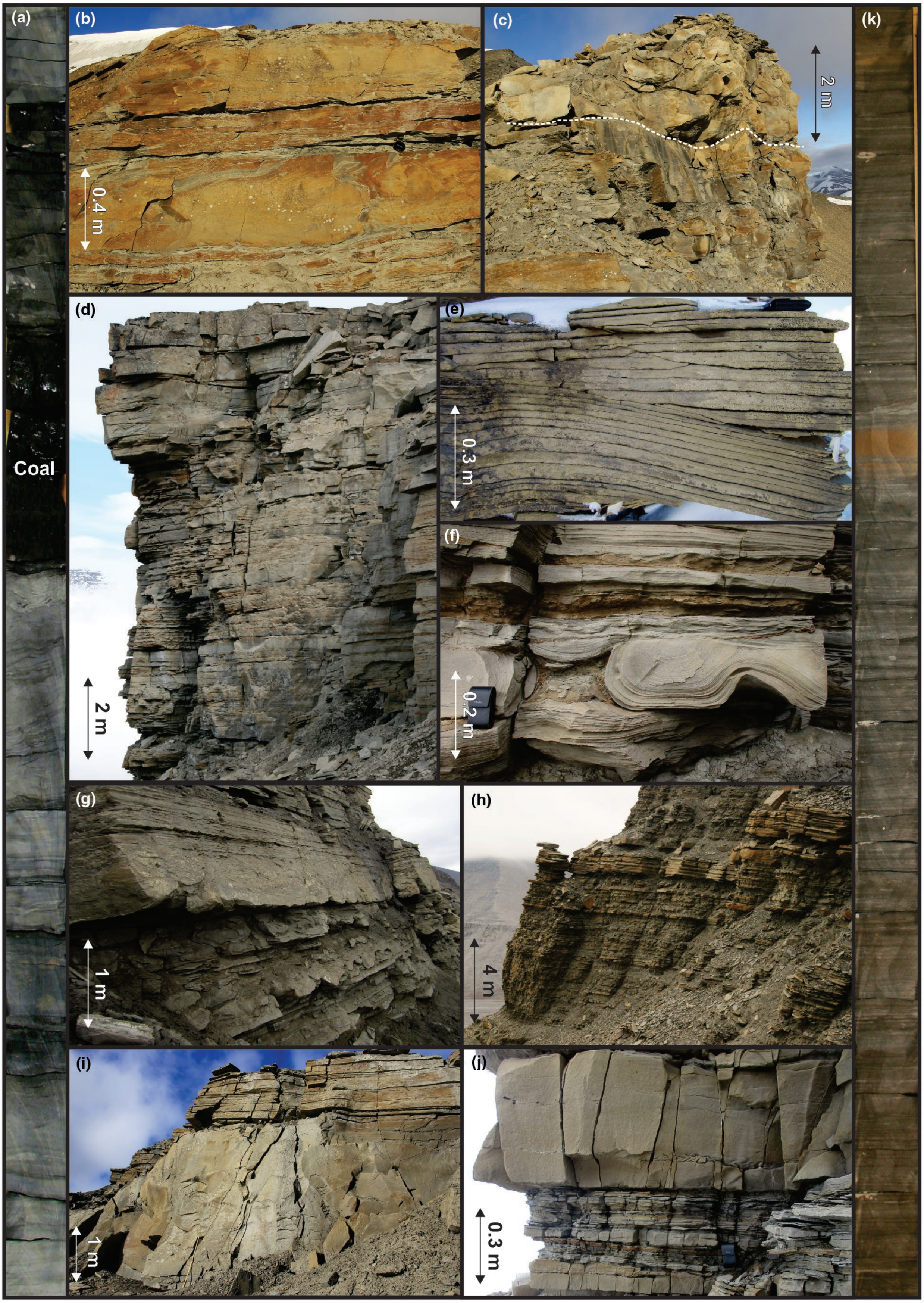
(a)
(b)
0.4 m
(c)
2 m
(k)
(d)
(e)
0.3 m
Coal
(f)
0.2 m
2 m
(g)
1 m
(h)
4 m
(i)
1 m
(j)
0.3 m

**FIGURE 7** Facies types from the different depositional systems in the GBA-unit (for locations of localities, see Figure 1): (a–c) fine-grained coastal plain succession with coal bed (cores from the Sysselmannbreen well) (a), overbank sandstone sheets (from Brogniartfjella) (b), and channel sandstone body (stippled base) incising its associated and underlying overbank sheet (from Brogniartfjella) (c). (d–f) shelf-delta successions showing a typical coarsening-upwards parasequence (from (Vengefjellet) (d), hummocky-cross-stratification (from Lars Hiertafjellet) (e) and ball-and-pillow structures which are common features within these parasequences (from Brogniartfjella) (f). (g) shelf-edge delta depositional system showing stacked beds of soft-sediment deformed sandstones overlain by a sharp-based sandstone unit (from Brogniartfjella). (h and i) slope lobe depositional system with heterolithic sandstones organized into a crude upwards coarsening unit (from Storvola) (h), and thick-bedded and amalgamated erosionally based turbidite channel in a middle slope setting (from Pallfjellet) (i). (j) basin floor depositional system with a small-scale thickening upward cycle consisting of a thick turbidite bed stacked on top of thinner turbidite beds. Such cycles internally characterize many of the turbidite lobes (from Hyrnestabben). (k) finely laminated basinal mudstones with laminations of siltstone (light coloured streaks), and siderite bands (rusty colour) (from Sysselmannbreen well)

and thickness of interbedded mudstone increases distally, thus forming thin-bedded, heterolithic sheet-like deposits on the lower slope and proximal basin floor (Plink-Björklund & Steel, 2005). Still, at some localities (e.g. Storvola, cf. Figure 1) the sandy slope lobes can be traced basinward and down-dip into the sandstone-dominated turbidite lobes (Figure 5a,e) within the basin floor depositional system (below) (Crabaugh & Steel, 2004; Petter & Steel, 2006).

The normally graded and tabular character of the sandstone beds, as well as the local occurrence of plane parallel lamination and current ripple cross-lamination, suggest deposition by low-density turbidity currents, which deposited much of their sediment load on the slope to form slope lobes (e.g. Petter & Steel, 2006; Plink-Bjorklund et al., 2001). The coarsening—and thickening-upward or fining- and thinning-upward is recording progradation and retrogradation or lateral switching of slope lobes, respectively (Petter & Steel, 2006). The landward increase in sandstone content and bed-set amalgamation, and the up-dip transition into fluvial-dominated mouth bars, suggests that the lobes were fed by gravity flows deriving from shelf-edge deltas (e.g. Mellere et al., 2002; Petter & Steel, 2006). The amalgamated character of these deposits points to deposition by sustained turbidity flows near the fluvial distributary mouths. Sandy slope lobe deposits have been discussed in more detail by Steel et al. (2000), Plink-Bjorklund et al. (2001), Mellere et al. (2002), Plink-Björklund and Steel (2005) and Petter and Steel (2006).

In addition, lens-shaped, erosionally based, thin-to thick-bedded fine- to coarse-grained sandstone bodies encapsulated within thicker mudstone intervals occurs within this depositional system (Figures 6g and 7i). The sandstone bodies are typically 4–10 m thick and depending on outcrop orientation 50–300 m wide, and pinches out both landward and basinward (Johannessen & Steel, 2005). Internally, some of the bodies are thin- to medium bedded and contain lateral accretion surfaces, but more commonly they are thick-bedded and amalgamated (Figure 7i; see also Johannessen & Steel, 2005), contain mud chips conglomerates and flute casts. Based on the erosive bases and lens-shaped geometries, and its stratigraphic position in a slope setting above turbidite lobes, these are interpreted as middle to lower slope channels (Johannessen & Steel, 2005). Slope channels have earlier been described in the south-eastern part of the study area by Johannessen and Steel (2005), Clark and Steel (2006), and Petter and Steel (2006).

### 2.4.1 | Regional distribution of shelf-edge delta and slope depositional systems

Shelf-edge delta and slope deposits are most evident in the western part of the basin where they readily can be identified as sandstone clinothems protruding downwards through finer grained sediments (Figure 4e). Clinothem gradients, when restored for tectonic tilt, range from 2–5°, and their relief from 150 m to 250 m (Mellere et al., 2002; Petter & Steel, 2006; Plink-Bjorklund et al., 2001). Albeit conspicuous features, the sandstone clinothems only constitutes a minor part of the slope depositional system; slope deposits are for the most part mudstone and siltstone dominated (Figures 6e and 9; Grundvåg, Johannessen, et al., 2014) in the western segment of the basin and entirely dominated by mudstone in the eastern segment (Figure 9). In outcrops the fine material will normally be scree-covered, but well data in both the western (Grundvåg, Johannessen, et al., 2014) and eastern parts (Osen, 2012) of the basin confirms the dominance of fine-grained material. Despite this mudstone-dominance, the presence of sandstone clinothems (and basin floor turbidite lobes, below) restricted to the western part of the basin (Figure 4e) is a clear expression of deep water and steep slopes in this part of the basin providing potential energy for mass-gravity processes (Helland-Hansen, 1992, 2010). The sandy channels that are also present within the slope depositional system further demonstrates the importance of transport of sandy material from shelf-edge deltas to the basin floor (Johannessen & Steel, 2005).

## 2.5 | Basin floor

The basin floor depositional system is dominated by a finely laminated mudstone succession, but also includes 2–10 km long and up to 60 m thick basinward thickening-thinning sandstone

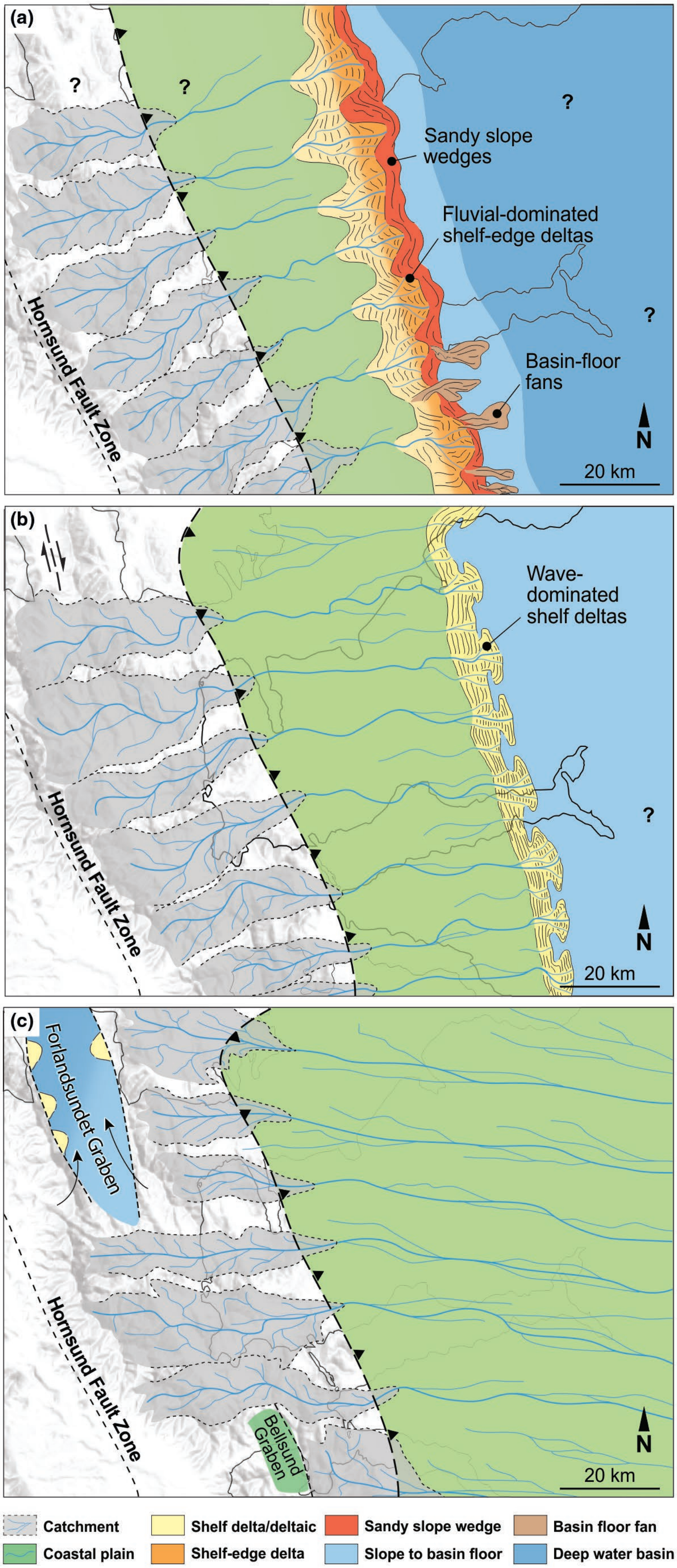


**FIGURE 8** Proposed paleogeographic maps for the GBA-unit at early stage of progradation when shorelines reaches local shelf-edges with accumulation of sandy slope wedges and basin-floor fans (a), when progradation has reached further into the shallower part of the basin (b) and finally, when the preserved part of the basin has been filled to sea-level with dominance of channel and inter-channel deposition (c). Paleocurrent measurements in fluvial channel deposits points to a slight southeasterly direction of outbuilding at the latter stage (cf. Helland-Hansen, 1990; Naurstad, 2014). Note that the Forlandsundet Graben could have been formed contemporaneously with the later stage of the filling of the Central Basin foredeep, in accordance with a late Eocene piggyback basin origin for this graben as proposed by Kleinspehn and Teyssier (2016). The same accounts for the Bellsund Graben which represent the southward extension of the Forlandsundet Graben (Blinova et al., 2009), although the age of the basin fill is debated (cf. Poole, 2018)

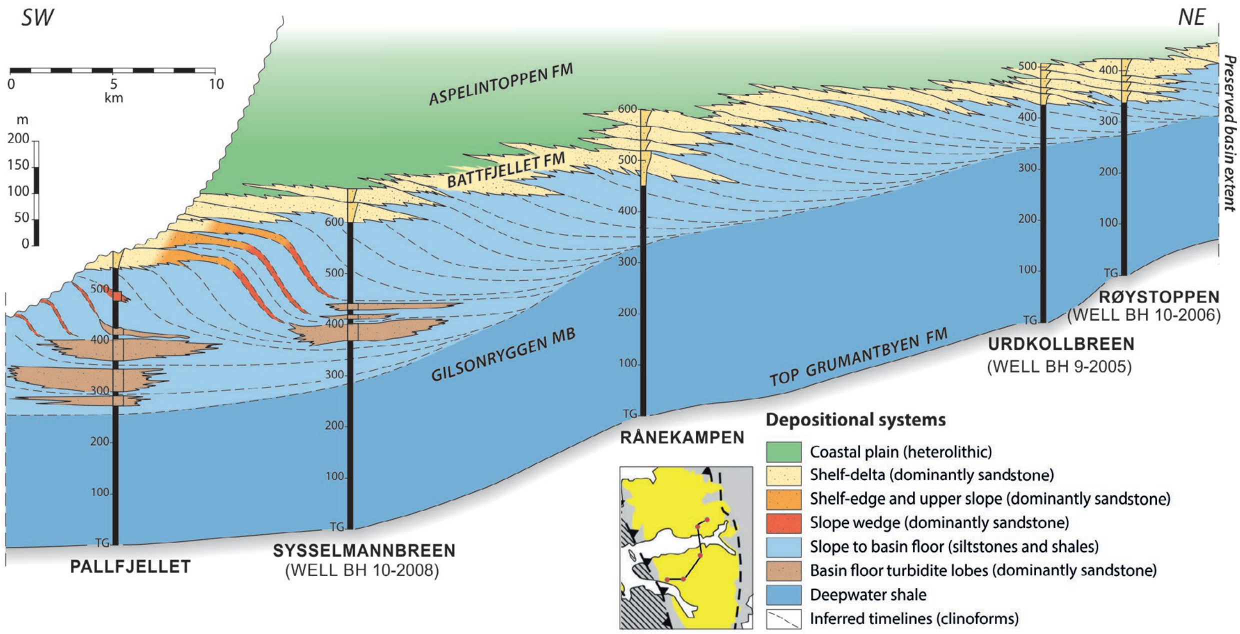


**FIGURE 9** Southwest-to-northeast transect through the Gilsonryggen Member, and Battfjellet and Aspelintoppen formations showing depositional systems and time-space development of the succession. Stippled lines are hypothesized timelines. Deliberately we have showed an ascending trajectory of the system emphasizing its overall stratigraphic climb. Note also the shingled architecture of the Battfjellet Formation, the common vertical termination of shelf parasequences in shallow-marine lithosomes (except the uppermost one that transitions into the Aspelintoppen Formation), the presence of shelf-edge delta, sandy slope and turbidite lobes of the basin floor depositional system limited to the western part of the basin and the gradual shallowing of the basin from west to east. Outline of insert map as for detailed map in Figure 1. Logs Pallfjellet and Sysselmannsbreen modified from Grundvåg, Johannessen, et al., 2014, log Rånekampen modified from Olsen, 2008, logs Urdkollbreen and Røystoppen modified from Osen, 2012)

wedges (Figure 6h,I; Crabaugh & Steel, 2004; Grundvåg, Johannessen, et al., 2014). These have a markedly lower depositional gradient than their associated and partly up-dip connected sandy slope lobe counterparts (Figure 5a,e). The wedges comprise alternating siltstone, heterolithic units and thin- to thick-bedded very fine- to medium- and subordinate coarse-grained sandstones (Figure 7j). The sandstone beds are generally normally graded, records basinward thinning and -fining, and occur as vertically stacked coarsening- and thickening-upward units, 1–12 m thick, with sheet-like geometries (Grundvåg, Johannessen, et al., 2014). Individual units are typically separated by siltstones or heterolithic intervals (Figure 6h,I). Locally, erosionally based, amalgamated thick-bedded sandstone units typically cap or incise the coarsening- and thickening-upward units (e.g. upper part of succession shown in Figure 6h; Grundvåg, Johannessen, et al., 2014). Basinward, the sheet-like units grades into heterolithic deposits. Detailed facies breakdown is given in Grundvåg, Johannessen, et al., 2014.

The sandstone-dominated part of this depositional system is interpreted as gravity-emplaced sandy deposits forming channelized turbidite lobe-complexes on the otherwise mudstone-dominated lower slope and basin floor (e.g. Clark & Steel, 2006; Crabaugh & Steel, 2004). Normally-graded sandstone beds that fine and thins basinward and locally comprises current-generated structures, indicates deposition from down-slope decelerating turbidity currents. Stacked coarsening- and thickening-upward successions represent prograding lobes and lobe elements (e.g. MacDonald, Peakall, Wignall, & Best, 2011; Prélat, Hodgson, & Flint, 2009). The heterolithics located basinward of these successions represent the lobe fringe (e.g. Hodgson et al., 2006).

### 2.5.1 | Regional distribution of basin floor depositional system

As for the slope depositional system, the sandstone dominated parts of the basin floor depositional system only has a clear outcrop expression in the western segment of the basin (Figure 4f and 10). In Nathorst Land (cf. Figure 1), turbidite lobe deposits apparently occur in two distinct zones trending NNW-*SSE* across the entire peninsula; the westernmost of these zones can be extended northwards to Nordenskiold Land (cf. Figure 1) (Figure 4f). Each zone is approximately 7–9 km wide and is present in the western and central parts of the basin. The easternmost limit of these deposits coincides with the eastern limit for the presence of sand-prone shelf-margin clinothems (Figure 4e), thus confirming the link between shelf-edge deltas and deep-water deposition (cf. Helland-Hansen, 2010; Johannessen & Steel, 2005). It might be speculated that the two documented zones with turbidite lobe deposits represent two pronounced episodes with basin-wide bypass of sand-grade sediments to the basin floor. In other foreland basins similar basin-floor gravity flow deposition have been interpreted to reflect deposition following periods of tectonically-induced hinterland uplift (e.g. Mutti, Tinterri, Benevelli, Di Biase, & Cavanna, 2003).

The basin floor sandstones are all encased in mudstones and siltstones (basin floor below, slope above) that less commonly crop out. In the eastern part of the basin, thicker basin floor sandstones are not evident in outcrops. This could partly be due to scree cover; however, well data in this region are devoid of turbidite lobe deposits supporting the notion of their absence in this area (Osen, 2012).

## 2.6 | Deepwater shale

Below the level of the basin floor turbidite lobes and down to the top of the Hollendardalen Formation in the western part of the basin and the Grumantbyen Formation further east (beyond the eastward pinchout of the Hollendardalen Formation, Figure 2), monotonous shales dominates, with thicknesses of about 300-370m in the western part of the basin (cf. well BH 10-2008, Sysselmannsbreen well, Grundvåg, Johannessen, et al., 2014; see also Steel et al., 1981). In the eastern part of the basin it is more difficult to estimate these thicknesses because basin floor deposits time equivalent to the turbidite lobe deposits in the western part of the basin are here mudstone dominated and hence, a datum for estimating sub-basin floor depositional system shale thicknesses is missing. Wells in the eastern part of the basin, west of Svea (BH 11-2003 and BH 10-2006), have shale thickness (from top Grumantbyen Formation to base Battfjellet Formation) ranging from 340 to 370 m (cf. Figure 9) (Osen, 2012), which is in the same order as the shale thickness *below* the turbidite lobes of the basin floor depositional system in the Sysselmannbreen well (BH 10-2008) at Nathorst Land (Grundvåg, Helland-Hansen, et al., 2014).

Facies-wise the mudstones are organic rich (total organic carbon 3%, Harding et al., 2011) and finely laminated (Figure 7k). They contain rare pin-striped laminations of siltstone, and concretions and siderite bands are common (Figure 7k). Siltstones and thin sandstones are increasing in frequency upwards towards the basin floor depositional system. The deposits reflect tranquil background deep-water pelagic or hemi-pelagic sedimentation out of reach from high-energetic processes (Grundvåg, Johannessen, et al., 2014).

# 3 | BASIN FILL OVERVIEW

## 3.1 | Linkage of depositional systems

Figure 9 shows a cross-sectional representation of the depositional systems discussed above in their relative stratigraphic position. Generally, the progradational GBA-unit shows a shingled time-transgressive architectural pattern of coastal plain to marine lithosomes all over the basin. As noted, individual shelf-delta parasequences generally show a tabular geometry at outcrop scale, an expression of a sand distribution being conditioned by the vertical energy-zonation in the water-column (Figure 9) (Helland-Hansen, 2010).

It is these parasequences that in the western basin-segment in a few instances are seen to peel off into discernible slope- and sometimes also basin floor turbidite lobes (Figure 5a,d,e and 10). Hence, both shelf-edge delta depositional system, sandy slope depositional system (together constituting clinothems) and turbidite lobes of the basin floor depositional system are restricted to the western part of the basin (Figure 4e,f). As pointed out in earlier publications (e.g. Helland-Hansen, 1990, 2010) this reflects higher subsidence rates and deeper water in the western basin-segment fostering steeper gradients and more potential energy for mass transport processes to funnel sediments beyond the "littoral energy fence" (Swift & Thorne, 1991) and into deeper water as opposed to the eastern segment where shallower waters persisted. For the same reason, we denote deltas that are fronted by deep (>150 m) waters and steep slope gradients in the western part of the basin "shelf-edge deltas" whereas deltas fronting shallow waters (tens of meters) for "shelf-deltas" (cf. Porębski & Steel, 2003). The latter type of delta is present both in the western and eastern part of the basin (Figure 9).

This west-east distinction is also expressed in the thickness map of the marine part of the Central Basin foredeep succession (combined Hollendardalen Formation and GBA-unit, Figure 4b); a clear westward thickening emphasizes the asymmetrical downwarping in front of the fold-and-thrust-belt. However, as can be speculated from the apparently relative uniform thickness of the deep water shale depositional system across the basin (below the basin-floor-turbidite-lobes in the western part of the basin, Figure 9), this downwarping may have been most pronounced in the later stage of the marine basin fill, specifically from the time of initiation of turbidite lobe deposition and onwards. Some uncertainty is attached to defining the sub basin floor thickness in the eastern part of the basin since the basin floor depositional system here is not clearly expressed. Still the lack of sandstone clinothems and turbidite lobes in this part of the basin points to shallower water than in the west during this stage of basin development with water depths more likely in the order of tens of meters. A development in compliance with the numerical models of Flemings and Jordan (1989) can be envisaged. They demonstrated an early thrust-sheet emplacement phase causing asymmetric subsidence towards the orogen (with only minor shoreline progradation), followed by shoreline progradation into the foredeep during post thrust-load-emplacement isostatic uplift. A similar two-stage tectonostratigraphic development can be inferred for the Hollendardalen

Formation (Figure 2) which shows a similar westerly thickening as the above-mentioned part of the GBA-unit.

The predominance of fine material in the GBA-unit as a whole (dominantly mudstones, siltstones and very fine- and fine-grained sandstones) with a virtual lack of conglomeratic material is a characteristic feature of the basin fill. Even within the most proximal coastal plain depositional system (the Aspelintoppen Formation) only the very basal parts of fluvial distributary channels include some conglomeratic material (Naurstad, 2014) and no sourceward increase in grain size is recorded. This suggests that coarser grained material was extracted closer to the source area beyond the current outcrop limits or, alternatively, that the source area did not yield coarser material which may seem likely owing to predominance of Late Paleozoic and Mesozoic rocks in the source area (cf. Petersen, Thomsen, Olaussen, & Stemmerik, 2016.). Nonetheless, from this it can be inferred that more proximal continental depositional environments (e.g. potential braidplains and alluvial fans) were still some distance away at the time of coastal plain deposition of the Aspelintoppen Formation across the area.

### 3.2 | Shelf-edge Trajectory

The system as a whole demonstrates a gradually ascending shelf-edge trajectory with successive shelf-edge and shelf deltas occupying successively stratigraphically higher positions as the system builds into the basin (cf. Deibert et al., 2003; Løseth, Steel, Crabaugh, & Schellpeper, 2006) (Figure 9). The overall ascending trajectory is punctuated by transgressive events (Figure 9), of which most are interpreted to be the effect of delta lobe shifting (Helland-Hansen, 2010). Grundvåg, Helland-Hansen, et al. (2014) calculated the average trajectory to be 0. 88° and 1.2°, based on correlations of the Battfjellet Formation along the south side of Van Mijenfjorden (36.5 km long transect) and north side of Van Keulenfjorden (22 km long transect), respectively. The thick succession of continental deposits of the Aspelintoppen Formation, 1 km maximum preserved thickness and in the order of ½ km removed (Marshall et al., 2015), indicates that the shorelines in front of the coastal and alluvial plains were climbing stratigraphically beyond the preserved limits of the basin, further to the east and possibly also to the south (see discussion below).

## 4 | DISCUSSION—CONTROLS ON BASIN FILL

### 4.1 | Basin type

The GBA-unit was laid down in the foredeep zone of a foreland basin system (sensu DeCelles & Giles, 1996) as evidenced by (a) the pronounced thickening of the succession towards the orogeny and (b) the absence of intraformational unconformities or progressive deformation. The basin probably extended far beyond the foredeep zone and beyond the outcrop limits towards the east. This is suggested from the absence of any evidence of basin margin deposits at the eastern margin of the basin and the presence the thick continental deposits of the Aspelintoppen Formation.

Syndepositional thrusting along decollement zones in the underlying Late Paleozoic and Mesozoic succession (Blinova, Faleide, Gabrielsen, & Mjelde, 2013; Braathen & Bergh, 1995) may have transformed the basin into a wedge-top basin in later stages of the basin filling. E.g. Blinova et al., 2013 indicates development of a decollement zone within Triassic shales contemporaneous with intense Eocene transpression; movement along this zone is likely to have coincided in time with basin filling. The pronounced westward thickening of the upper marine part of the succession (Figure 4b) points to a foredeep rather than a wedge-top setting, however, it cannot be excluded that the transformation into a wedge-top basin took place contemporaneous with the deposition of the continental Aspelintoppen Formation or during deposition of the sediments that have later been eroded. Gentle structuring on the basin floor producing swells and troughs may have formed already during the emplacement of the basin floor fans. This is suggested by apparent north to northeastward-directed palaeocurrent indicators (i.e. flute casts and tool marks) in some of the submarine fan bodies (Crabaugh & Steel, 2004). Alternatively, this may be explained in terms of increased lateral spreading of turbidity flows as they move across an unconfined basin floor (cf. large spread in palaeocurrent directions in eastern part of basin, Figure 4f).

The Svalbard foreland basin is anomalous in the sense that it is bordered by a transpressive orogeny and is as such classified as a transpressional basin (Ingersoll, 1988). Transform movements is evidenced by the regional picture as well as the present structural configuration (Bergh & Grogan, 2003; Doré, Lundin, Gibbons, Sømme, & Tørudbakken, 2015; Faleide et al., 1993, 2008; Kristensen et al., 2018; Steel et al., 1985). The predominantly western input recorded in the succession strongly reflects ongoing shortening and uplift in the west; however, evidence of strike-slip in the sedimentary succession, such as lateral migration of depocenters and lateral offsets of matched provenance areas and deposits (Nilsen & Sylvester, 1999), has not been demonstrated. The absence of evidence for the strike-slip regime in the succession could simply be an expression of the length of the studied segment of the foreland basin relative to the full strike extent of the orogeny, preventing signs of strike-slip to be recorded in the sedimentary succession. In addition, prolonged partitioning into strike-slip and compression (Braathen & Bergh, 1995; Leever, Gabrielsen, Faleide, & Braathen, 2011) would prevent strike-slip signals to be recorded in the basin fill. It should be noted that Piepjohn et al. (2016) favoured a model with early Eocene compression followed by dextral transpression as well as transtension in the late Eocene. Determining the age of the basin stratigraphy would be critical in correlating sedimentation with tectonic style for such a complex tectono-stratigraphic development.

An integral part of foreland basins is the peripheral bulge (DeCelles & Giles, 1996). We suggest that the thinning we see towards the east is an expression of deposition on the flank of the peripheral bulge. There is no evidence to suggest that the bulge was elevated above sea-level since neither regional erosion nor reversal of sediment routing is evident in the more distal part of the succession (cf. Bruhn & Steel, 2003).

The present day Hornsund Fault Zone off the Svalbard margin, about 50km west of the present day Central Basin axis, may have been close to the axis of the shear-zone between Greenland and Svalbard (Eldholm, Faleide, & Myhre, 1987) and it is reasonable to assume that the drainage divide was not located west of this. Hence, the source area was probably relatively close (few tens of kilometers) to the basin. From established scaling relationships between drainage area and catchment length (Hack, 1957; Helland-Hansen, Grundvåg, & Aadland, 2017), we assume that the catchments that fed the foreland basin was relatively small; 500–1,000 km$^2$ (Figure 8).

## 4.2 | Basin forming processes

The thickness (<2 km) and width (<50 km) of the Svalbard foredeep succession is moderate relative to what is typical for compressional foredeep depozones (typically 2–8 km thick and 100-300 km wide, DeCelles & Giles, 1996). The anomalous low thickness and width may be typical for transpressional foredeeps; these are normally less than 100 km wide (c.f. de Urreiztieta, Gapais, Le Corre, Cobbold, & Rossello, 1996; Eichhubl, Greene, & Maher, 2002; Meng, Wang, & Hu, 2005). A factor that may play a role in defining the limited width and amplitude of the transpressional foredeeps could be shearing along the transform margin partitioning the crust also within the foredeep zone. The main effect of lateral change in the lithosphere, such as disruptions by strike-slip motions, would be to increase the amplitude of the foredeep at the expense of reducing the width (Beaumont, Keen, & Boutilier, 1982).

Alternatively, the shallow depth and short wave-length could be an expression of crustal buckling rather than flexural downwarping. Zhang and Bott (2000) proposed a model of plastic compressional folding as an alternative to the supracrustal loading model for foreland basin development. However, their modelling generated much deeper basins than what is recorded in the Svalbard foredeep. Criteria to identify flexural loading includes a significant depth and thickening of foreland basin successions close to the thrust front and accompanying rapid tapering towards the craton and minor amplitudes in deflection beyond the forebulge. Buckling on the other hand tends to form repeated gentle anticlines and synclines at long distances (≫1,000 km) away from the orogeny (Allen & Allen, 2013).

Although these considerations are based on settings of pure compression and not necessarily directly applicable to transpressive settings, we believe that the pronounced thickening of the basin fill towards the orogen (Figure 7b) is an expression of dominance of downflexing rather than buckling. However, thin-skinned partitioned shortening involving buckling cannot be excluded as an additional process. The thickness map of the Central Basin foredeep succession (Figure 4b) demonstrates NW-SE trending isopachs with thickening towards the SW. This trend is oblique to the present NNW-SSE structural grain of the WSFTB and could be an expression partitioned shortening related to the right-lateral oblique motions along the margin (cf. Sanderson & Marchini, 1984). This is also in agreement with the Eocene NE-SW crustal shortening proposed by Braathen, Bergh, & Maher, 1999 (their stage 4–5). It should be noted that Kristensen et al. (2018) demonstrated a depocenter oblique to the sheared margin in the Sørvestsnaget Basin along the Senja Shear Margin (Figure 1), a southwards extension of the Svalbard Margin in the Barents Sea. This depocenter also have an Eocene infill with a similar counter-clockwise isopach obliquity (20–30°) to the Senja Shear Margin as the Central Basin foredeep succession has to the Svalbard Margin. However, this basin is much narrower (ca. 5 km, Central Basin close to 50 km) and is related to crustal buckling associated with a transtensional regime (Kristensen et al., 2018).

The observed obliquity between the isopachs (Figure 4b) and the WSFTB/Central Basin axis may indicate basin deepening towards the south. No southwards directed axial (along orogen) sediment transport has been recorded in the basin fill. However, as shown in Figure 4e, the eastern limit of clinothems are located closer to the orogen in the southern part of the basin than in the north. This could be a sedimentary response to southwards basin deepening.

The presumably maximum removed overburden in the Central Basin based on vitrinite reflectance data in the coals of the Firkanten Formation (Manum & Throndsen, 1978; cf. also Marshall et al., 2015) coincides with the present axis of the Central Basin. Hence, the depocenter of the Aspelintoppen Formation and eroded deposits is eastwards offset not only to the marine part of the GBA-unit, but also relative to the depocenter of the older Paleogene formations (cf. Bruhn & Steel, 2003) and may point to an eastward and cratonward migrating depocenter (Helland-Hansen, 1990).

### 4.3 | Subsidence and eustasy

Dörr et al., 2013 performed a backstripping and subsidence analysis of the post-Devonian sedimentary succession of Svalbard. In their one-dimensional backstripping they arrived at an average subsidence rate (including isostatic and compactional subsidence) for Van Mijenfjorden Group at 0.04 mm/year (1 km over 25 my, cf. their Figure 4). It is reasonable to suggest that subsidence rates were significantly higher than average during the deposition of the upper marine succession (from level of basin floor turbidite lobes and through the Battfjellet Formation and time-equivalent Aspelintoppen Formation deposits) due to significant downflexing of the crust associated with the climax of the WSFTB. Subsidence rates where highest in the western orogen-flanking part of the basin and decreased towards the craton.

We compared the average subsidence rate of Dörr et al., 2013 with rates derived from the eustatic sea-level curve of Miller et al., 2005 for the Eocene. Several major falls have rates exceeding 0.04 mm/year, included the very pronounced early Eocene (52, 8–51 my) eustatic fall with an amplitude of 79 m and an average fall-rate of 0.044 mm/year. At least 5 longer periods within the Eocene have significant sea-level falls with average rates exceeding 0.04 mm/year. Maximum rates for 100 000-year periods exceeds 0.1 mm/year 16 times. However, one should keep in mind the gravitational attraction that the supracrustal load of the WSFTB exerted on the sea-level; this would cause higher than average sea-level and hence, subdued effect of potential eustatic sea-level falls (cf. Haq, 2014).

The question is whether potential relative sea-level falls can be identified in the studied succession. Several papers have suggested repeated episodes of relative sea-level falls (frequently below shelf-edge) (Mellere et al., 2002; Plink-Bjorklund et al., 2001; Plink-Björklund & Steel, 2002), and interpret incised valleys from sedimentological criteria (Mellere et al., 2003; Plink-Björklund, 2005; Plink-Björklund & Steel, 2006). For example, Plink-Björklund and Steel (2006) identified three incised valleys within the coastal plain succession (i.e. the Aspelintoppen Formation) at Brogniartfjella (location in Figure 1) with an estimated fluvial downcutting of 26 m, 57 m and 67 m, respectively. The two deeply cut valleys apparently resulted from relative sea-level falls below the shelf edge, eventually resulting in slope bypass and the development of coeval basin-floor fans (Plink-Björklund & Steel, 2006). In addition, the same authors interpret subaerial unconformities and associated wave-cut terraces on the upper part of the Högsnyta slope wedge (location in Figure 1), again advocating fall of sea level below shelf edge (Plink-Björklund & Steel, 2002). Grundvåg, Helland-Hansen, et al., 2014 on the other hand, states that there is no clear evidence of any significant basinward facies dislocations or erosional unconformities within the Battfjellet Formation based on data from Nathorst Land (including Brogniartfjella, see figs 9 and 11 in Grundvåg, Helland-Hansen, et al., 2014). Grundvåg, Helland-Hansen, et al. (2014), do however, recognize the presence of erosively-based distributary channel fills cut down into their associated delta front facies, and incised upper slope to shelf-edge channel complexes whose origin is debatable (e.g. retrogressive slumping, see Steel et al., 2000). Relative sea-level falls imply significant eustatic falls to counteract the typically high rates of foreland basin subsidence (cf. Allen & Allen, 2013). Literature discussing relative sea-level changes within the foredeep zones generally favour absence of relative sea falls: subsidence rates in foreland basins has been argued to invariably exceed the rate of eustatic falls in areas proximal to the orogenic belt, but only sporadically in regions distal to the thrust load (Bera, Sarkar, Chakraborty, Loyal, & Sanyal, 2008; Castle, 2001; Escalona & Mann, 2006; Hoy & Ridgway, 2003; Posamentier & Allen, 1993; Willis, 2000).

As noted above, a major element in the basin filling style is the shingled appearance of the coastal plain to shallow marine lithosomes and the highly variable number of shelf-deltas over short distances (Figure 4c and 10). This has been attributed to an elongate morphology of the deltas with pronounced delta-lobe shifting, each lobe-shift and accompanying flooding producing intervals of fine-material deposition (Grundvåg, Helland-Hansen, et al., 2014; Helland-Hansen, 1992). Still, it can be questioned whether all finer-grained levels (typically separating the cliff-forming sandstones) should be attributed to lobe-shifting. Some fine-grained units are seen to produce thicker and more laterally extensive ledges along the mountainsides and may represent events of relative sea-level rise of more widespread nature than what can be produced from more local flooding events emanating from shifting of delta-lobes. In light of the proposed high subsidence rates in combination with recurrent eustatic sea-level rises it seems easier to argument for major events of relative sea-level rise than for relative sea-level fall.

### 4.4 | Sediment supply

Sediment was primarily derived from the west as evidenced by paleocurrent data across the basin as well as the direction of sloping and thinning of clinothems in the western part of the basin (Figure 4e,f). In addition, provenance studies confirm a western source area for the GBA-unit (e.g. Petersen et al., 2016). Notable is the nearly uniform N-S orientation of wave ripple crests across the basin (Figure 4d) and current generated structures at the delta front and basin mostly have easterly directions (Figure 4e,f) (Grundvåg, Helland-Hansen, et al., 2014; Helland-Hansen, 1990). Wave-ripple crests typically align parallel to the coast (Potter & Pettijohn, 1963) and correspond well with the easterly directed current generated structures and the eastwards sloping clinoforms, together indicating eastwards advancing deltas.

The west to east transport direction is oblique to the NW-SE isopach trend. Isopachs in overfilled basins (Hadler-Jacobsen et al., 2005) reflect long-term spatial variations in subsidence. However, progradational elements of such systems, in this case delta progadation, may simply "ignore" slow and long-term subsidence and subsidence-variations simply from the fact that progradation across the basin is a rapid process compared to subsidence. Tectonic basin subsidence is <0.5 mm/year for most basin types (Allen & Allen, 2013) whereas delta progradation is a measure of meters to hundreds of meters per year (Aadland & Helland-Hansen, 2016), explaining the mismatch between transport directions and isopach trends. In this case, the isopach trends would basically demonstrate spatially varying subsidence rates recorded by slowly and vertically accreted intervals (e.g. deep-water shales).

Several sedimentological criteria indicate temporally high sedimentation rates. The pervasive soft sediment deformation at multiple levels (Grundvåg, Helland-Hansen, et al., 2014; Helland-Hansen, 2010; Naurstad, 2014; Steel et al., 1981), particularly in heterolithic successions, points to rapid deposition, subsequent dewatering and accompanying deformation. Much of this soft sediment deformation is seen to be caused by vertical foundering rather than lateral down-slope movement (evidenced by predominance of ball-and-pillow and other loading structures relative to structures caused by slumping) (Grundvåg, Helland-Hansen, et al., 2014; Helland-Hansen, 2010). The lower heterolithic part of the Battfjellet Formation, the heterolithic (inter-channel) successions in the Aspelintoppen Formation and fluvial sandbodies in the Aspelintoppen Formation are the levels with most frequent soft sediment deformation structures. In the slope wedges, the abundance of thick-bedded hyperpycnal turbidite beds rich in plant material indicate the presence of high-supply shelf-edge deltas (Plink-Björklund & Steel, 2005). The high degree of bed amalgamation in the turbidite lobes, as well as their progradational stacking also indicates a high supply system (Grundvåg, Johannessen, et al., 2014). In addition, the immature character of the sediment with poor sorting and abundance of unstable fragments (including organic detritus and shale fragments) (cf. Helland-Hansen, 2010) suggests rapid deposition and little time for winnowing of sediments, even in the shallow marine domain.

## 4.5 | Basin extent

How far south and east did the basin extend? It is known from seismic studies in the western and SW Barents Shelf that a large middle Eocene-Oligocene clinoform system shed significant amounts of sediments into the deeper parts of the Vestbakken Volcanic Province and the Sørvestsnaget Basin (cf. Figure 1) (e.g. Lasabuda, Laberg, Knutsen, & Safronova, 2018; Rasmussen, Skott, & Larsen, 1995; Ryseth et al., 2003; Safronova, Henriksen, Andreassen, Laberg, & Vorren, 2014). Specifically, Safronova et al., 2014 reported southwards prograding clinoform systems of middle Eocene age in the Sørvestsnaget Basin and proposed that these were sourced from the Stappen High. The latter feature was uplifted in the early Eocene as a response first to shearing and later rift flank uplift as this segment of the Northernmost Atlantic separated from the Greenland margin (Gabrielsen, Faerseth, Jensen, Kalheim, & Riis, 1990). It is likely that the Stappen High was connected to the WSFTB and that a coastline run from the Central Basin and southwards to the eastern flank of the Stappen High (Bergh & Grogan, 2003). According to Smelror, Petrov, Larssen, and Werner (2009) this sea was narrow in the Svalbard area extending south with its eastern shores in the immediate vicinity of the present-day eastern margin of the Central Basin. Further south, towards 76°N, the sea is indicated with an eastern branch. We believe that his sea extended much further eastwards also in the Central Basin area. The dominantly eastward directed paleocurrent directions in the GBA-unit throughout the basin, suggests that the drainage did not orient southwards during the time encompassed by the preserved marine and continental infill. However, it should be noted that paleocurrent data in fluvial channel-fills of the Aspelintoppen Formation commonly have southeasterly directions, which may indicate early clockwise rotation of drainage patterns (cf. Figure 7c). Potential feeding of sediments to the western and SW Barents Shelf would have been routed farther east and southeast and beyond the present day Central Basin eastern margin before turning south. A possible peripheral bulge east of the present Central Basin margin may have been instrumental in this southwards sediment diversion. Although speculations, a southwards sediment transport may also have been important along the Central Basin during the deposition of the younger foreland basin fill that later was eroded.

## 5 | CONCLUSIONS

The post early Eocene Gilsonryggen Member, Battfjellet Formation and Aspelintoppen Formation together formed an eastwards prograding succession (> 1 km thick) filling the foreland of the West Spitsbergen fold-and-thrust belt. The catchments were small (500–1,000 km$^2$) and the distance to the source terrain and probably also the drainage divide was short (tens of kilometers). The succession consists of coastal plain, shelf delta, shelf-edge delta, slope, basin floor and deepwater shale depositional systems with shelf-edge deltas, slope clinothems and basin floor fans being restricted to the western and deepest part of the basin. The system prograded with an ascending trajectory around

1° and it is expected that this trend also persisted beyond the preserved outcrop belt, explaining the considerable thickness (>1 km) of the continental deposits capping the progradational package. The progradational architecture demonstrates an extremely shingled character with limited lateral extent (3–6 km) of basinward offset shallow-marine lithosomes. The sediment supply rate was intermittently high as evidenced by immaturity of the rocks and the pervasive soft sediment deformation and probably is a reflection of the proximity to the source area. Sediments accumulated in a foredeep zone of a foreland basin system with subsidence driven by flexural loading potentially accompanied by crustal buckling. From the high-subsidence foredeep setting it can be assumed that subsidence outpaced eustatic sea-level falls and that episodes of relative sea-level falls were few. The system may have been connected to contemporaneous progradational systems west and south of the Stappen High further south, however, evidence of southwards sediment routing is not evident in the system.

## ACKNOWLEDGMENTS

Thanks to Tore Aadland and Atle Rotevatn who gave constructive feedback to parts of earlier versions of this manuscript and to journal reviewers Cornel Olariu and Per Terje Osmundsen. Eva Bjørseth drafted Figures 8 and 9. Sten-Andreas Grundvåg received funding from the ARCEx project (Research Centre for Arctic Petroleum Exploration), which is funded by the Research Council of Norway (grant number 228107).

## CONFLICT OF INTEREST

None.

## PEER REVIEW

The peer review history for this article is available at https://publons.com/publon/10.1111/bre.12492.

## DATA AVAILABILITY STATEMENT

The data that support the findings of this study are available from the corresponding author upon reasonable request.

## ORCID

*William Helland-Hansen* https://orcid.org/0000-0002-7529-1485

## REFERENCES

Aadland, T., & Helland-Hansen, W. (2016). Global compilation of coastline change at river mouths. In *EGU General Assembly Conference Abstracts*, *18*, p. 3915.

Aamelfot, T. (2019). *Sedimentology of the Battfjellet Formation, Liljevalchfjellet, Svalbard* (p. 102). MSc thesis. Bergen, Norway: University of Bergen.

Allen, P. A., & Allen, J. R. (2013). *Basin analysis: Principles and application to petroleum play assessment* (p. 327). Hoboken, NJ: John Wiley & Sons.

Atkinson, D. J. (1963). Tertiary rocks of Spitsbergen. *American Association of Petroleum Geologists Bulletin*, *47*, 302–323.

Beaumont, C., Keen, E., & Boutilier, R. (1982). A comparison of foreland and rift margin sedimentary basins. *Philosophical Transactions of the Royal Society of London, A*, *305*, 295–317.

Bera, M., Sarkar, A., Chakraborty, P., Loyal, R., & Sanyal, P. (2008). Marine to continental transition in Himalayan foreland. *Geological Society of America Bulletin*, *120*, 1214–1232. https://doi.org/10.1130/B26265.1

Bergh, S. G., Braathen, A., & Andresen, A. (1997). Interaction of basement-involved and thin-skinned tectonism in the Tertiary fold-thrust belt of central Spitsbergen, Svalbard. *American Association of Petroleum Geologists Bulletin*, *81*, 637–661.

Bergh, S. G., & Grogan, P. (2003). Tertiary structure of the Sørkapp-Hornsund Region, South Spitsbergen, and implications for the offshore southern extension of the fold-thrust Belt. *Norwegian Journal of Geology*, *83*, 43–60.

Birkenmajer, K., & Narebski, W. (1963). Dolerite drift blocks in marine Tertiary of Sørkapp Land and some remarks on the geology of the eastern part of this area. *Norsk Polarinstitutt Årbok*, *1962*, 68–79.

Blinova, M., Faleide, J. I., Gabrielsen, R. H., & Mjelde, R. (2013). Analysis of structural trends of sub-sea-floor strata in the Isfjorden area of the West Spitsbergen Fold-and-Thrust Belt based on multichannel seismic data. *Journal of the Geological Society*, *170*, 657–668. https://doi.org/10.1144/jgs2012-109

Blinova, M., Thorsen, R., Mjelde, R., & Faleide, J. I. (2009). Structure and evolution of the Bellsund Graben between Forlandsundet and Bellsund (Spitsbergen) based on marine seismic data. *Norwegian Journal of Geology*, *89*, 215–228.

Braathen, A., & Bergh, S. G. (1995). Kinematics of Tertiary deformation in the basement-involved fold-thrust belt, western Nordenskiold Land, Svalbard: Tectonic implications based on fault slip data analysis. *Tectonophysics*, *249*, 1–29.

Braathen, A., Bergh, S. G., & Maher, J. H. D. (1999). Application of a critical wedge taper model to the Tertiary transpressional fold-thrust belt on Spitsbergen, Svalbard. *Geological Society of America Bulletin*, *111*, 1468–1485.

Broze, E. (2017). *The occurrence of flow transformations within sandy submarine fans: A case study from the Eocene on Spitsbergen* (p. 147). MSc thesis. Tromsø, Norway: University of Tromsø.

Bruhn, R., & Steel, R. (2003). High-resolution sequence stratigraphy of a clastic foredeep succession (Paleocene, Spitsbergen): An example of peripheral-bulge-controlled depositional architecture. *Journal of Sedimentary Research*, *73*, 745–755. https://doi.org/10.1306/012303730745

Castle, J. W. (2001). Foreland-basin sequence response to collisional tectonism. *Geological Society of America Bulletin*, *113*, 801–812. https://doi.org/10.1130/0016-7606(2001)113<0801:FBSRTC>2.0.CO;2

Charles, A. J., Condon, D. J., Harding, I. C., Pälike, H., Marshall, J. E. A., Cui, Y., … Croudace, I. W. (2011). Constraints on the numerical age of the Paleocene-Eocene boundary. *Geochemistry, Geophysics, Geosystems*, *12*, 1–19. https://doi.org/10.1029/2010GC003426

Clark, B. E., & Steel, R. J. (2006). Eocene turbidite-population statistics from shelf edge to basin floor, Spitsbergen, Svalbard. *Journal of Sedimentary Research*, *76*, 903–918. https://doi.org/10.2110/jsr.2006.078

Clifton, A. (2012). *The Eocene flora of Svalbard and its climatic significance* (p. 401). PhD thesis. Leeds, UK: University of Leeds.

Crabaugh, J. P., & Steel, R. J. (2004). Basin-floor fans of the Central Tertiary Basin, Spitsbergen; relationship of basin-floor sand-bodies to prograding clinoforms in a structurally active basin. In S. A. Lomas, & P. Joseph (Eds.), *Confined turbidite systems* (Vol. *222*, pp. 187–208). London: Geological Society, Special Publications.

Dalland, A. (1977). Erratic clasts in the Lower Tertiary deposits of Svalbard—Evidence of transport by winter ice. *Norsk Polarinstitutt Årbok*, *1976*, 151–165.

Dallmann, W. K. (1999). *Lithostratigraphic Lexicon of Svalbard* (p. 318). Tromsø, Norway: Committee on the Stratigraphy of Svalbard/ Norsk Polarinstitutt.

Dallmann, W. K., & Elvevold, S. (2015). Bedrock geology. In W. K. Dallmann (Ed.), *Geoscience atlas of Svalbard*, Tromsø, Norway: Report Series. Norwegian Polar Institute.

De Urreiztieta, M., Gapais, D., Le Corre, C., Cobbold, P., & Rossello, E. (1996). Cenozoic dextral transpression and basin development at the southern edge of the Puna Plateau, northwestern Argentina. *Tectonophysics*, *254*, 17–39. https://doi.org/10.1016/0040-1951(95)00071-2

DeCelles, P. G., & Giles, K. A. (1996). Foreland basin systems. *Basin Research*, *8*, 105–123. https://doi.org/10.1046/j.1365-2117.1996.01491.x

Deibert, J. E., Benda, T., Løseth, T., Schellpeper, M., & Steel, R. J. (2003). Eocene clinoform growth in front of a storm-wave-dominated shelf, Central Basin, Spitsbergen: No significant sand delivery to deepwater areas. *Journal of Sedimentary Research*, *73*, 546–558. https://doi.org/10.1306/011703730546

Dimakis, P., Braathen, B. I., Faleide, J. I., Elverhøi, A., & Gudlaugsson, S. T. (1998). Cenozoic erosion and the preglacial uplift of the Svalbard-Barents Sea region. *Tectonophysics*, *300*, 311–327. https://doi.org/10.1016/S0040-1951(98)00245-5

Doré, A. G., Lundin, E. R., Gibbons, A., Sømme, T. O., & Tørudbakken, B. O. (2015). Transform margins of the Arctic: A synthesis and re-evaluation. In M. Nemcok, S. Rybar, S. T. Sinha, S. A. Hermeston, & L. Ledvenyiova (Eds.), *Transform margins: Development, controls and petroleum systems* (Vol. *431*, pp. 63–94). London: Geological Society, Special Publication.

Dörr, N., Clift, P. D., Lisker, F., & Spiegel, C. (2013). Why is Svalbard an island? Evidence for two-stage uplift, magmatic underplating, and mantle thermal anomalies. *Tectonics*, *32*, 473–486. https://doi.org/10.1002/tect.20039

Dörr, N., Lisker, F., Jochmann, M., Rainer, T., Schlegel, A., Schubert, K., & Spiegel, C. (2019). Subsidence, rapid inversion, and slow erosion of the Central Tertiary Basin of Svalbard: Evidence from the thermal evolution and basin modeling. In K. Piepjohn, J. V. Strauss, L. Reinhardt, & W. C. McClelland (Eds.), *Circum-arctic structural events: Tectonic evolution of the arctic margins and trans-arctic links with adjacent orogens* (*Series paper: 541*, pp. 169–189). Boulder, CO: Geological Society of America.

Eichhubl, P., Greene, H. G., & Maher, N. (2002). Physiography of an active transpressive margin basin: High-resolution bathymetry of the Santa Barbara basin, Southern California continental borderland. *Marine Geology*, *184*, 95–120. https://doi.org/10.1016/S0025-3227(01)00280-8

Eldholm, O., Faleide, J. I., & Myhre, A. M. (1987). Continent-ocean transition at the western Barents Sea/Svalbard continental margin. *Geology*, *15*, 1118–1122. https://doi.org/10.1130/0091-7613(1987)15<1118:CTATWB>2.0.CO;2

Eldholm, O., Sundvor, E., Myhre, A. M., & Faleide, J. L. (1984). Cenozoic evolution of the continental margin of Norway and western Svalbard. In A. M. Spencer (Ed.), *Petroleum geology of the north European margin* (pp. 3–18). London: Graham & Trotman.

Escalona, A., & Mann, P. (2006). Sequence-stratigraphic analysis of Eocene clastic foreland basin deposits in central Lake Maracaibo using high-resolution well correlation and 3-D seismic data. *American Association of Petroleum Geologists Bulletin*, *90*, 581–623. https://doi.org/10.1306/10130505037

Faleide, J. I., Tsikalas, F., Breivik, A. J., Mjelde, R., Ritzmann, O., Engen, O., … Eldholm, O. (2008). Structure and evolution of the continental margin off Norway and the Barents Sea. *Episodes*, *31*, 82–91. https://doi.org/10.18814/epiiugs/2008/v31i1/012

Faleide, J. I., Vågenes, E., & Gudlaugsson, S. T. (1993). Late Mesozoic-Cenozoic evolution of the southwestern Barents Sea. *Geological Society, London, Petroleum Geology Conference Series*, *4*, 933–950. https://doi.org/10.1144/0040933

Flemings, P. B., & Jordan, T. E. (1989). A synthetic stratigraphic model of foreland basin development. *Journal of Geophysical Research - Solid Earth*, *94*, 3851–3866. https://doi.org/10.1029/JB094iB04p03851

Forman, S. L., Lubinski, D. J., Miller, G. H., Snyder, J., Matishov, G. G., Korsun, S., & Myslivets, V. (1995). Postglacial emergence and distribution of Late Weichselian ice-sheet loads in the northern Barents and Kara Seas, Russia. *Geology*, *23*, 113–116. https://doi.org/10.1130/0091-7613(1995)023<0113:PEADOL>2.3.CO;2

Gabrielsen, R. H., Faerseth, R. B., Jensen, L. N., Kalheim, J. E., & Riis, F. (1990). Structural elements of the Norwegian continental shelf. Pt. 1. The Barents Sea region. Norwegian Petroleum Directorate Bulletin, *6*, 33.

Gaina, C., Gernigon, L., & Ball, P. (2009). Palaeocene-Recent plate boundaries in the NE Atlantic and the formation of the Jan Mayen microcontinent. *Journal of the Geological Society*, *166*, 601–616. https://doi.org/10.1144/0016-76492008-112

Gjelberg, H. K. (2010). *Facies Analysis and Sandbody Geometry of the Paleogene Battfjellet Formation, Central Western Nordenskiöld Land, Spitsbergen* (p. 174), MSc thesis. Bergen, Norway: University of Bergen.

Golovneva, L. (2010). Variability in epidermal characters of Ginkgo tzagajanica Samylina (Ginkgoales) from the Paleocene of the Tsagayan Formation (Amur region) and the taxonomy of Tertiary species of Ginkgo. *Paleontological Journal*, *44*, 584–594. https://doi.org/10.1134/S003103011005014X

Greenwood, D. R., Basinger, J. F., & Smith, R. Y. (2010). How wet was the Arctic Eocene rain forest? Estimates of precipitation from Paleogene Arctic macrofloras. *Geology*, *38*, 15–18. https://doi.org/10.1130/G30218.1

Grundvåg, S.-A., Helland-Hansen, W., Johannessen, E. P., Olsen, A. H., & Stene, S. A. K. (2014). The depositional architecture and facies variability of shelf deltas in the Eocene Battfjellet Formation, Nathorst Land, Spitsbergen. *Sedimentology*, *61*, 2172–2204. https://doi.org/10.1111/sed.12131

Grundvåg, S.-A., Johannessen, E. P., Helland-Hansen, W., & Plink-Björklund, P. (2014). Depositional architecture and evolution of progradationally stacked lobe complexes in the Eocene Central Basin of Spitsbergen. *Sedimentology*, *61*, 535–569. https://doi.org/10.1111/sed.12067

Hack, J. T. (1957). *Studies of longitudinal stream profiles in Virginia and Maryland*. U.S. Geological Survey Professional Paper, 294-B.

Hadler-Jacobsen, F., Johannessen, E., Ashton, N., Henriksen, S., Johnson, S., & Kristensen, J. (2005). Submarine fan morphology and lithology distribution: A predictable function of sediment delivery, gross shelf-to-basin relief, slope gradient and basin topography. *Geological Society, London, Petroleum Geology Conference Series*, *6*, 1121–1145. https://doi.org/10.1144/0061121

Haq, B. U. (2014). Cretaceous eustasy revisited. *Global and Planetary Change*, *113*, 44–58. https://doi.org/10.1016/j.gloplacha.2013.12.007

Harding, I. C., Charles, A. J., Marshall, J. E. A., Pälike, H., Roberts, A. P., Wilson, P. A., … Akbari, S. (2011). Sea-level and salinity fluctuations during the Paleocene-Eocene thermal maximum in Arctic Spitsbergen. *Earth and Planetary Science Letters*, *303*, 97–107. https://doi.org/10.1016/j.epsl.2010.12.043

Harland, W. B., Anderson, L. M., Manasrah, D., & Butterfield, N. J. (1997). *The Geology of Svalbard* (Vol. *17*). London: Geological Society of London, Memoir.

Helland-Hansen, W. (1985). *Sedimentology of the Battfjellet Formation (Palaeogene) in Nordenskiold Land, Spitsbergen* (p. 322), Cand.scient. thesis. Bergen, Norway: University of Bergen.

Helland-Hansen, W. (1990). Sedimentation in Paleogene foreland basin, Spitsbergen. *American Association of Petroleum Geologists Bulletin*, *74*, 260–272.

Helland-Hansen, W. (1992). Geometry and facies of Tertiary clinothems, Spitsbergen. *Sedimentology*, *39*, 1013–1029. https://doi.org/10.1111/j.1365-3091.1992.tb01994.x

Helland-Hansen, W. (2010). Facies and stacking patterns of shelf-deltas within the Palaeogene Battfjellet Formation, Nordenskiöld Land, Svalbard: Implications for subsurface reservoir prediction. *Sedimentology*, *57*, 190–208.

Helland-Hansen, W., Grundvåg, S. A., & Aadland, T. (2017). Assessment of duration of basin filling without chronostratigraphic data: A case study from the Cenozoic foreland basin of Spitsbergen. *International Meeting of Sedimentology* 2017, Toulouse (abstract).

Helland-Hansen, W., Helle, H. B., & Sunde, K. (1994). Seismic modeling of Tertiary sandstone clinothems, Spitsbergen. *Basin Research*, *6*(4), 181–191. https://doi.org/10.1111/j.1365-2117.1994.tb00084.x

Hodgson, D. M., Flint, S. S., Hodgetts, D., Drinkwater, N. J., Johannessen, E. P., & Luthi, S. M. (2006). Stratigraphic evolution of fine-grained submarine fan systems, Tanqua depocenter, Karoo Basin, South Africa. *Journal of Sedimentary Research*, *76*, 20–40. https://doi.org/10.2110/jsr.2006.03

Hoy, R. G., & Ridgway, K. D. (2003). Sedimentology and sequence stratigraphy of fan-delta and river-delta deposystems, Pennsylvanian Minturn Formation, Colorado. *American Association of Petroleum Geologists Bulletin*, *87*, 1169–1191. https://doi.org/10.1306/03110300127

Ingersoll, R. V. (1988). Tectonics of sedimentary basins. *Geological Society of America Bulletin*, *100*, 1704–1719. https://doi.org/10.1130/0016-7606(1988)100<1704:TOSB>2.3.CO;2

Jochmann, M. M., Augland, L. E., Lenz, O., Bieg, G., Haugen, T., Grundvåg, S. A., … Hjálmarsdóttir, H. R. (2019). Sylfjellet: A new outcrop of the Paleogene Van Mijenfjorden Group in Svalbard. *Arktos*, 1–22. https://doi.org/10.1007/s41063-019-00072-w

Johannessen, E. P., Henningsen, T., Bakke, N. E., Johansen, T. A., Ruud, B. E., Riste, P., … Woldengen, M. S. (2011). Palaeogene clinoform succession on Svalbard expressed in outcrops, seismic data, logs and cores. *First Break*, *29*(2), 35–44. https://doi.org/10.3997/1365-2397.2011004

Johannessen, E. P., & Steel, R. J. (2005). Shelf-margin clinoforms and prediction of deepwater sands. *Basin Research*, *17*, 521–550. https://doi.org/10.1111/j.1365-2117.2005.00278.x

Johansen, S., Granberg, E., Mellere, D., Arntsen, B., & Olsen, T. (2007). Decoupling of seismic reflectors and stratigraphic timelines: A modeling study of Tertiary strata from Svalbard. *Geophysics*, *72*(5), SM273–SM280. https://doi.org/10.1190/1.2759479

Jones, M. T., Augland, L. E., Shephard, G. E., Burgess, S. D., Eliassen, G. T., Jochmann, M. M., … Svensen, H. H. (2017). Constraining shifts in North Atlantic plate motions during the Palaeocene by U-Pb dating of Svalbard tephra layers. *Scientific Reports*, *7*(1), 1–9. https://doi.org/10.1038/s41598-017-06170-7

Jørgensen, K. W. (2015). *Sedimentology of inter-channel deposits of the Aspelintoppen Formation, Brogniartfjella, Svalbard* (p. 72). MSc thesis. Bergen, Norway: University of Bergen.

Kellogg, H. E. (1975). Tertiary stratigraphy and tectonism in Svalbard and continental drift. *American Association of Petroleum Geologists Bulletin*, *59*, 465–485.

Kleinspehn, K. L., & Teyssier, C. (2016). Oblique rifting and the Late Eocene-Oligocene demise of Laurasia with inception of Molloy Ridge: Deformation of Forlandsundet Basin, Svalbard. *Tectonophysics*, *693*, 363–377. https://doi.org/10.1016/j.tecto.2016.05.010

Knies, J., Matthiessen, J., Vogt, C., Laberg, J. S., Hjelstuen, B. O., Smelror, M., … Vorren, T. O. (2009). The Plio-Pleistocene glaciation of the Barents Sea-Svalbard region: A new model based on revised chronostratigraphy. *Quaternary Science Reviews*, *28*, 812–829. https://doi.org/10.1016/j.quascirev.2008.12.002

Kongsgården, A. G. (2016). *Sedimentology of channel-deposits of the Aspelintoppen Formation, Brogniartfjella, Svalbard* (p. 98). MSc thesis. Bergen, Norway: University of Bergen.

Kristensen, T. B., Rotevatn, A., Marvik, M., Henstra, G. A., Gawthorpe, R. L., & Ravnås, R. (2018). Structural evolution of sheared margin basins: The role of strain partitioning. Sørvestsnaget Basin, Norwegian Barents Sea. *Basin Research*, *30*, 279–301. https://doi.org/10.1111/bre.12253

Kvaček, Z. (1994). Connecting links between the Arctic Palaeogene and European Tertiary floras. In M. C. Boulter, & H. C. Fisher (Eds.), *Cenozoic plants and climates of the Arctic*, NATO ASI Series, I (Vol. *27*, pp. 251–266). Berlin, Heidelberg, Germany: Springer.

Landvik, J. Y., Bondevik, S., Elverhøi, A., Fjeldskaar, W., Mangerud, J., Salvigsen, O., … Vorren, T. O. (1998). The last glacial maximum of Svalbard and the Barents Sea area: Ice sheet extent and configuration. *Quaternary Science Reviews*, *17*, 43–75. https://doi.org/10.1016/S0277-3791(97)00066-8

Lasabuda, A. P. E., Laberg, J. S., Knutsen, S.-M., & Safronova, P. (2018). Cenozoic tectonostratigraphy and pre-glacial erosion: A mass-balance study of the northwestern Barents Sea margin. *Journal of Geodynamics*, *119*, 149–166.

Leever, K. A., Gabrielsen, R. H., Faleide, J. I., & Braathen, A. (2011). A transpressional origin for the West Spitsbergen fold-and-thrust belt: Insight from analog modeling. *Tectonics*, *30*(2), 1–24. https://doi.org/10.1029/2010TC002753

Løseth, T. M., Steel, R. J., Crabaugh, J. P., & Schellpeper, M. (2006). Interplay between shoreline migration paths, architecture and pinchout distance for siliciclastic shoreline tongues: Evidence from the rock record. *Sedimentology*, *53*, 735–767. https://doi.org/10.1111/j.1365-3091.2006.00791.x

Lundin, E., & Doré, A. (2002). Mid-Cenozoic post-breakup deformation in the ‘passive’margins bordering the Norwegian-Greenland Sea. *Marine and Petroleum Geology*, *19*, 79–93. https://doi.org/10.1016/S0264-8172(01)00046-0

Macdonald, H. A., Peakall, J., Wignall, P. B., & Best, J. (2011). Sedimentation in deep-sea lobe-elements: Implications for the origin of thickening-upward sequences. *Journal of Geological Society*, *168*, 319–332. https://doi.org/10.1144/0016-76492010-036

Major, H., & Nagy, J. (1972). Geology of the Adventdalen map area: With a geological map, Svalbard C9G 1: 100 000. *Norsk Polarinstitutt Skrifter*, *138*, 1–58.

Mansurbeg, H., Morad, S., Plink-Bjorklund, P., El-Ghali, M. A. K., Caja, M. A., & Marfil, R. (2012). Diagenetic alterations related to falling stage and lowstand systems tracts of shelf, slope and basin floor sandstones (Eocene Central Basin, Spitsbergen). *International Association of Sedimentologists Special Publication*, *45*, 353–378.

Manum, S. B., & Throndsen, T. (1978). Rank of coal and dispersed organic matter and its geological bearing in the Spitsbergen Tertiary. *Norsk Polarinstitutt Årbok*, *1977*, 159–177.

Manum, S. B., & Throndsen, T. (1986). Age of Tertiary formations on Spitsbergen. *Polar Research*, *4*, 103–131. https://doi.org/10.1111/j.1751-8369.1986.tb00526.x

Marshall, C., Uguna, J., Large, D. J., Meredith, W., Jochmann, M., Friis, B., … Orheim, A. (2015). Geochemistry and petrology of palaeocene coals from Spitzbergen—Part 2: Maturity variations and implications for local and regional burial models. *International Journal of Coal Geology*, *143*, 1–10. https://doi.org/10.1016/j.coal.2015.03.013

Mellere, D., Breda, A., & Steel, R. J. (2003). Fluvially incised shelf-edge deltas and linkage to upper-slope channels (Central Tertiary Basin, Spitsbergen). In N. C. R. H. H. Roberts, R. H. Fillon, & J. B. Anderson (Eds.), *Shelf-Margin Deltas and Linked downslope Petroleum Systems*, (pp. 231–266, CD-ROM). Gulf Coast Section SEPM 23rd Annual Research Conference Proceedings.

Mellere, D., Plink-Bjorklund, P., & Steel, R. (2002). Anatomy of shelf deltas at the edge of a prograding Eocene shelf margin, Spitsbergen. *Sedimentology*, *49*, 1181–1206. https://doi.org/10.1046/j.1365-3091.2002.00484.x

Meng, Q.-R., Wang, E., & Hu, J.-M. (2005). Mesozoic sedimentary evolution of the northwest Sichuan basin: Implication for continued clockwise rotation of the South China block. *Geological Society of America Bulletin*, *117*, 396–410. https://doi.org/10.1130/B25407.1

Miller, K. G., Kominz, M. A., Browning, J. V., Wright, J. D., Mountain, G. S., Katz, M. E., … Pekar, S. F. (2005). The Phanerozoic record of global sea-level change. *Science*, *310*, 1293–1298. https://doi.org/10.1126/science.1116412

Müller, R. D., & Spielhagen, R. F. (1990). Evolution of the Central Tertiary Basin of Spitsbergen: Towards a synthesis of sediment and plate tectonic history. *Palaeogeography, Palaeoclimatology, Palaeoecology*, *80*(2), 153–172. https://doi.org/10.1016/0031-0182(90)90127-S

Mutti, E., Davoli, G., Tinterri, R., & Zavala, C. (1996). The importance of ancient fluvio-deltaic systems dominated by catastrophic flooding in tectonically active basins. *Memorie Di Scienze Geologiche*, *48*, 233–291.

Mutti, E., Tinterri, R., Benevelli, G., Di Biase, D., & Cavanna, G. (2003). Deltaic, mixed and turbidite sedimentation of ancient foreland basins. *Marine and Petroleum Geology*, *20*, 733–755. https://doi.org/10.1016/j.marpetgeo.2003.09.001

Nathorst, A. G. (1910). Beiträge zur Geologie der Bären-Insel, Spitzbergens und des König-Karl-Landes. *Bulletin of the Geological Institution of the University of Uppsala*, *10*, 261–415.

Naurstad, O. A. (2014). *Sedimentology of the Aspelintoppen Formation (Eocene-Oligocene), Brogniartfjella, Svalbard* (p. 124), MSc thesis. Bergen, Norway: University of Bergen.

Nilsen, T. H., & Sylvester, A. G. (1999). Strike-slip basins: Part 1. *The Leading Edge*, *18*, 1146–1152. https://doi.org/10.1190/1.1438170

Nysæther, E. (1966). *Petrografisk undersøkelse av sedimentære bergarter fra tidsperioden kritt-tertiær i Nathorst Land* (p. 168). Cand. Real. Thesis. Bergen, Norway: University of Bergen.

Olsen, A. (2008). *Sedimentology and paleogeography of the Battfjellet Fm. Southern Van Mijenfjorden, Svalbard* (p. 91). MSc thesis. Bergen, Norway: University of Bergen.

Osen, T. G. (2012). *Facies, Sandbody Geometry and Palaeogeography of the Battfjellet Formation, Urdkolldalen area, Nordenskiold Land, Svalbard* (p. 90). MSc thesis. Bergen, Norway: University of Bergen.

Petersen, T. G., Thomsen, T., Olaussen, S., & Stemmerik, L. (2016). Provenance shifts in an evolving Eurekan foreland basin: The Tertiary Central Basin, Spitsbergen. *Journal of the Geological Society*, *173*, 634–648. https://doi.org/10.1144/jgs2015-076

Petter, A. L., & Steel, R. J. (2006). Hyperpycnal flow variability and slope organization on an Eocene shelf margin, Central Basin, Spitsbergen. *American Association of Petroleum Geologists Bulletin*, *90*, 1451–1472. https://doi.org/10.1306/04240605144

Piepjohn, K., von Gosen, W., & Tessensohn, F. (2016). The Eurekan deformation in the Arctic: An outline. *Journal of the Geological Society*, *173*, 1007–1024. https://doi.org/10.1144/jgs2016-081

Plink-Björklund, P. (2005). Stacked fluvial and tide-dominated estuarine deposits in high-frequency (fourth-order) sequences of the Eocene Central Basin, Spitsbergen. *Sedimentology*, *52*, 391–428. https://doi.org/10.1111/j.1365-3091.2005.00703.x

Plink-Bjorklund, P., Mellere, D., & Steel, R. J. (2001). Turbidite variability and architecture of sand-prone, deep-water slopes: Eocene clinoforms in the Central Basin, Spitsbergen. *Journal of Sedimentary Research*, *71*, 895–912. https://doi.org/10.1306/030501710895

Plink-Björklund, P., & Steel, R. J. (2002). Sea-level fall below the shelf edge, without basin-floor fans. *Geology*, *30*(2), 115–118. https://doi.org/10.1130/0091-7613(2002)030<0115:SLFBTS>2.0.CO;2

Plink-Björklund, P., & Steel, R. (2005). Deltas on falling-stage and lowstand shelf margins, the Eocene Central Basin of Spitsbergen: Importance of sediment supply. *SEPM Special Publication*, *83*, 179–206.

Plink-Björklund, P., & Steel, R. (2006). Incised valleys on an Eocene coastal plain and shelf, Spitsbergen—Part of a linked shelf–slope system. *SEPM Special Publication*, *85*, 281–307.

Ponten, A., & Plink-Björklund, P. (2009). Process regime changes across a regressive to transgressive turnaround in a shelf-slope basin, Eocene Central Basin of Spitsbergen. *Journal of Sedimentary Research*, *79*, 2–23. https://doi.org/10.2110/jsr.2009.005

Poole, L. K. (2018). *Sedimentology of the Paleogene succession at Calypsostranda, Svalbard* (p. 159). MSc thesis. Bergen, Norway: University of Bergen.

Porębski, S. J., & Steel, R. J. (2003). Shelf-margin deltas: Their stratigraphic significance and relation to deepwater sands. *Earth-Science Reviews*, *62*(3–4), 283–326. https://doi.org/10.1016/S0012-8252(02)00161-7

Posamentier, H., & Allen, G. (1993). Siliciclastic sequence stratigraphic patterns in foreland, ramp-type basins. *Geology*, *21*, 455–458. https://doi.org/10.1130/0091-7613(1993)021<0455:SSSPIF>2.3.CO;2

Potter, P., & Pettijohn, F. (1963). *Paleocurrents and basin analysis* (p. 296). New York: Academic Press Inc.

Prélat, A., Hodgson, D., & Flint, S. (2009). Evolution, architecture and hierarchy of distributary deep-water deposits: A high-resolution outcrop investigation from the Permian Karoo Basin, South Africa. *Sedimentology*, *56*, 2132–2154. https://doi.org/10.1111/j.1365-3091.2009.01073.x

Rasmussen, E., Skott, P. H., & Larsen, K.-B. (1995). Hydrocarbon potential of the Bjørnøya West Province, western Barents Sea Margin. *Norwegian Petroleum Society Special Publication*, *4*, 277–286.

Ryseth, A., Augustson, J. H., Charnock, M., Haugerud, O., Knutsen, S.-M., Midbøe, P. S., … Sundsbø, G. (2003). Cenozoic stratigraphy and evolution of the Sørvestsnaget Basin, southwestern Barents Sea. *Norwegian Journal of Geology*, *83*, 107–130.

Safronova, P. A., Henriksen, S., Andreassen, K., Laberg, J. S., & Vorren, T. O. (2014). Evolution of shelf-margin clinoforms and deep-water fans during the middle Eocene in the Sorvestsnaget Basin, southwest Barents Sea. *American Association of Petroleum Geologists Bulletin*, *98*, 515–544.

Sanderson, D. J., & Marchini, W. (1984). Transpression. *Journal of Structural Geology*, *6*, 449–458. https://doi.org/10.1016/0191-8141(84)90058-0

Schlegel, A., Lisker, F., Dörr, N., Jochmann, M., Schubert, K., & Spiegel, C. (2013). Petrography and geochemistry of siliciclastic rocks from the Central Tertiary Basin of Svalbard – Implications for provenance, tectonic setting and climate. *Zeitschrift Der Deutschen Gesellschaft Für Geowissenschaften*, *164*, 173–186. https://doi.org/10.1127/1860-1804/2013/0012

Skarpeid, S. S. (2010). *Facies Architecture and Paleogeography of the Battfjellet Formation, Rypefjellet, Spitsbergen* (p. 113), MSc thesis. Bergen, Norway: University of Bergen.

Skjærpe, K. T. (2017). *Sedimentological facies analyses of Clinothem 8C (Eocene), Battfjellet Formation, Brogniartfjella, Svalbard* (p. 109), MSc thesis. Bergen, Norway: University of Bergen.

Smelror, M., Petrov, O., Larssen, G. B., & Werner, S. (2009). *Atlas: Geological history of the Barents Sea* (p. 135). Trondheim, Norway: Norges Geologiske Undersøkelse.

Steel, R. J. (1977). Observations on some Cretaceous and Tertiary sandstone bodies in Nordenskiöld Land. *Svalbard, Norsk Polarinstitutt Årbok*, *1976*, 43–68.

Steel, R. J., Crabaugh, J. P., Schellpeper, M., Mellere, D., Plink-Bjorklund, P., Deibert, J., & Løseth, T. M. (2000). Deltas versus rivers on the shelf edge: their relative contributions to the growth of shelf margins and basin-floor fans (Barremian and Eocene, Spitsbergen). In P. Weimer, R. M. Slatt, J. Coleman, N. C. Rosen, H. Nelson, A. H. Bouma, M. J., … Lawrence (Eds.), *Deep-water reservoirs of the world* (pp. 981–1009). Gulf Coast Section SEPM 20th Annual Research Conference Proceedings.

Steel, R., Dalland, A., Kalgraff, K., & Larsen, V. (1981). The Central Tertiary Basin of Spitsbergen: Sedimentary development of a Sheared-Margin Basin. In J. W. Kerr, & A. J. Ferguson (Eds.), *Geology of the North Atlantic Borderland* (Vol. *7*, pp. 647–664). Calgary, Canada: Canadian Society of Petroleum Geologists Memoir.

Steel, R., Gjelberg, J., Helland-Hansen, W., Kleinspehn, K., Nøttvedt, A., & Rye-Larsen, M. (1985). The Tertiary strike-slip basins and orogenic belt of Spitsbergen. *SEPM Special Publication*, *37*, 339–359.

Steel, R. J., & Olsen, T. (2002). Clinoforms, Clinoform Trajectories and Deepwater Sands. In J. M. Armentrout, & N. C. Rosen (Eds.), *Sequence stratigraphic models for exploration and production: Evolving methodology, emerging models and application histories* (pp. 367–381, CD-ROM). Gulf Coast Section SEPM 22th Annual Research Conference Proceedings.

Stene, S. A. K. (2008). *Facies and architecture of the Battfjellet Formation, northern Nathorst Land, Spitsbergen* (p. 103). MSc thesis. Bergen, Norway: University of Bergen.

Swift, D. J. P., & Thorne, J. A. (1991). Sedimentation on continental margins, I: a general model for shelf sedimentation. In D. J. P. Swift, G. F. Oertel, R. W. Tillman, & J. A. Thorne (Eds.) *Shelf sand and sandstone bodies: Geometry, facies and sequence stratigraphy*, Int. Assoc. Sedimentol. Spec. Publ., 14, 3–31.

Tegner, C., Storey, M., Holm, P. M., Thorarinsson, S., Zhao, X., Lo, C.-H., & Knudsen, M. F. (2011). Magmatism and Eurekan deformation in the High Arctic Large Igneous Province: 40 Ar–39 Ar age of Kap Washington Group volcanics, North Greenland. *Earth and Planetary Science Letter*, *303*, 203–214. https://doi.org/10.1016/j.epsl.2010.12.047

Uhl, D., Traiser, C., Griesser, U., & Denk, T. (2007). Fossil leaves as palaeoclimate proxies in the Palaeogene of Spitsbergen (Svalbard). *Acta Palaeobotanica Krakow*, *47*, 89.

Uroza, C. A., & Steel, R. J. (2008). A highstand shelf-margin delta system from the Eocene of West Spitsbergen, Norway. *Sedimentary Geology*, *203*, 229–245. https://doi.org/10.1016/j.sedgeo.2007.12.003

Van Wagoner, J. C., Mitchum, R. M., Campion, K. M., & Rahmanian, V. D. (1990). Siliciclastic sequence stratigraphy in well logs, cores, and outcrops: Concepts for high resolution correlation of time and facies. *American Association of Petroleum Geologists, Methods in Exploration Series*, *7*, 55.

Willis, A. (2000). Tectonic control of nested sequence architecture in the Sego Sandstone, Neslen Formation and upper Castlegate Sandstone (Upper Cretaceous), Sevier foreland basin, Utah, USA. *Sedimentary Geology*, *136*, 277–317. https://doi.org/10.1016/S0037-0738(00)00087-7

Zhang, G.-B., & Bott, M. H. (2000). Modelling the evolution of asymmetrical basins bounded by high-angle reverse faults with application to foreland basins. *Tectonophysics*, *322*, 203–218. https://doi.org/10.1016/S0040-1951(00)00104-9

## SUPPORTING INFORMATION

Additional supporting information may be found online in the Supporting Information section.

**How to cite this article:** Helland-Hansen W, Grundvåg S-A. The Svalbard Eocene-Oligocene (?) Central Basin succession: Sedimentation patterns and controls. *Basin Res*. 2021;33:729–753. https://doi.org/10.1111/bre.12492